

NPS 67-82-007

NAVAL POSTGRADUATE SCHOOL

Monterey, California



THESIS

FLOW CONTROL ABOUT AN
AIRBORNE LASER TURRET

by

Larry Ellis Penix

June 1982

Thesis Advisor:

A. E. Fuhs

Approved for public release; distribution unlimited

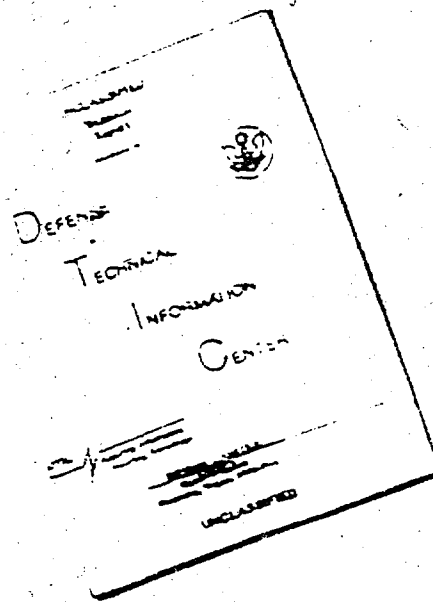
Air Force Weapons Laboratory/ARLB
Kirtland AFB
Albuquerque, NM 87177

DTIC
ELECTIC
JAN 10 1983

83 01 10 057 E

FILE COPY

DISCLAIMER NOTICE



THIS DOCUMENT IS BEST
QUALITY AVAILABLE. THE COPY
FURNISHED TO DTIC CONTAINED
A SIGNIFICANT NUMBER OF
PAGES WHICH DO NOT
REPRODUCE LEGIBLY.

REPRODUCED FROM
BEST AVAILABLE COPY

NAVAL POSTGRADUATE SCHOOL
Monterey, California 93940

Rear Admiral J. J. Ekelund
Superintendent

David Schradly
Acting Provost

This thesis prepared in conjunction with research supported in part by
Code ARLB, Air Force Weapons Laboratory, Kirtland AFB, New Mexico.
Reproduction of all or part of this report is authorized.

Released as a
Technical Report by:



W. M. Tolles
Dean of Research

UNCLASSIFIED

SECURITY CLASSIFICATION OF THIS PAGE (When Data Entered)

REPORT DOCUMENTATION PAGE		READ INSTRUCTIONS BEFORE COMPLETING FORM
1. REPORT NUMBER NPS 67-82-007	2. GOVT ACCESSION NO. AD-A223056	3. RECIPIENT'S CATALOG NUMBER
4. TITLE (and Subtitle) Flow Control About an Airborne Laser Turret		5. TYPE OF REPORT & PERIOD COVERED Master's thesis; June 1982
7. AUTHOR(s) Larry Ellis Penix		6. PERFORMING ORG. REPORT NUMBER NPS 67-82-007
8. PERFORMING ORGANIZATION NAME AND ADDRESS Naval Postgraduate School Monterey, California 93940		6. CONTRACT OR GRANT NUMBER(s) MIPR 82-MP-075
11. CONTROLLING OFFICE NAME AND ADDRESS Air Force Weapons Laboratory/ARLB Kirtland AFB, Albuquerque, NM 87177		10. PROGRAM ELEMENT, PROJECT, TASK AREA & WORK UNIT NUMBERS 62317J 63605F
14. MONITORING AGENCY NAME & ADDRESS (if different from Controlling Office)		12. REPORT DATE June 1982
		13. NUMBER OF PAGES 58
		14. SECURITY CLASS. (of this report) Unclassified
		15a. DECLASSIFICATION/DOWNGRADING SCHEDULE
16. DISTRIBUTION STATEMENT (of this Report) Approved for public release; distribution unlimited.		
17. DISTRIBUTION STATEMENT (of the abstract entered in Block 20, if different from Report)		
18. SUPPLEMENTARY NOTES		
19. KEY WORDS (Continue on reverse side if necessary and identify by block number) Airflow Control Laser Propagation Laser Turret Small Fairing		
20. ABSTRACT (Continue on reverse side if necessary and identify by block number) This thesis project is the latest in a series of experiments conducted at the Naval Postgraduate School to improve the air flow in which a laser beam propagates. The particular turret to be studied is currently employed on Airborne Laser Laboratory which is aboard the NKC-135 aircraft; a one-third scale model was constructed in the 5 x 5 foot wind tunnel. The objective is to decrease the optical path distortion and jitter resulting		

DD FORM 1 JAN 73 1473

EDITION OF 1 NOV 66 IS OBSOLETE
S. N. 0102-014-8601

UNCLASSIFIED

SECURITY CLASSIFICATION OF THIS PAGE (When Data Entered)

✓ #20 - ABSTRACT - (CONTINUED)

from turbulent flow in the aft hemisphere of the turret that houses the laser telescope. ✓

Afterbody fairing and fuselage boundary layer suction were employed with porous material added when necessary to stabilize the air flow. Compared to previous tests, the fairing was considerably smaller. Further, asymmetric arrangements consisting of an offset fairing were tested. A test matrix was developed that varied the fairing and base suction positions. Minimum suction duct velocity required to obtain quiescent flow was determined in each case. The lowest minimum flow for any configuration was 0.36 for the one-half offset condition.

The concept of using afterbody suction as a means of providing flow control with a geometrically smaller fairing than previously tested has proven effective for incompressible flow at critical Reynolds Number and low velocity.

Accession For	
NTIS GRA&I	<input checked="" type="checkbox"/>
DTIC TAB	<input type="checkbox"/>
Unannounced	<input type="checkbox"/>
Justification	<input type="checkbox"/>
By	
Distribution/	
Availability Codes	
Dist	Avail and/or Special
A	



Approved for public release; distribution unlimited.

Flow Control About an
Airborne Laser Turret

by

Larry Ellis Penix
Lieutenant Commander, United States Navy
B.S., The Ohio State University, 1971

Submitted in partial fulfillment of the
requirements for the degree of

MASTER OF SCIENCE IN ENGINEERING SCIENCE

from the

NAVAL POSTGRADUATE SCHOOL

June 1982

Author:

Larry E. Penix

Approved by:

John A. Collins
Thesis Advisor

Daniel J. Collins
Chairman, Department of Aeronautics

William M. Miller
Dean of Science and Engineering

ABSTRACT

This thesis project is the latest in a series of experiments conducted at the Naval Postgraduate School to improve the air flow in which a laser beam propagates. The particular turret to be studied is currently employed on Airborne Laser Laboratory which is aboard the NKC-135 aircraft; a one-third scale model was constructed in the 5 x 5 foot wind tunnel. The objective is to decrease the optical path distortion and jitter resulting from turbulent flow in the aft hemisphere of the turret that houses the laser telescope.

Afterbody fairing and fuselage boundary layer suction were employed with porous material added when necessary to stabilize the air flow. Compared to previous tests, the fairing was considerably smaller. Further, asymmetric arrangements consisting of an offset fairing were tested. A test matrix was developed that varied the fairing and base suction positions. Minimum suction duct velocity required to obtain quiescent flow was determined in each case. The lowest minimum flow for any configuration was 0.36 for the one-half offset condition.

The concept of using afterbody suction as a means of providing flow control with a geometrically smaller fairing than previously tested has proven effective for incompressible flow at critical Reynolds Number and low velocity.

TABLE OF CONTENTS

I.	INTRODUCTION -----	10
	A. BACKGROUND -----	10
	B. THESIS OBJECTIVE -----	13
II.	FLOW CONTROL -----	14
	A. THEORY -----	14
	B. DISCUSSION OF PRESSURE COEFFICIENT -----	15
	C. METHOD OF FLOW CONTROL -----	16
III.	EXPERIMENTAL APPARATUS -----	17
	A. PHYSICAL COMPONENTS -----	17
	B. INSTRUMENTATION -----	18
IV.	EXPERIMENTAL RESULTS -----	20
	A. TEST PROCEDURE -----	20
	B. RESULTS -----	21
V.	CONCLUSIONS -----	26
	APPENDIX A: PRESSURE COEFFICIENT CALCULATION -----	53
	APPENDIX B: SUCTION DUCT VOLTAGE-TO-VELOCITY CONVERSION EQUATIONS -----	54
	LIST OF REFERENCES -----	55
	INITIAL DISTRIBUTION LIST -----	57

LIST OF TABLES

I.	PRESSURE TAP--SCANIVALVE LOCATIONS -----	51
II.	SUMMARY OF RESULTS -----	52

LIST OF FIGURES

1.	TURRET PRESSURE TAP LOCATIONS -----	27
2.	THEORETICAL PRESSURE DISTRIBUTION FOR A SPHERE AND CYLINDER -----	28
3.	LASER TURRET, FAIRING, AND WIND TUNNEL CONFIGURATION -----	29
4.	FUSELAGE BLEED SLOT, FORWARD, SIDE, AND AFT -----	30
5.	FAIRING DIMENSIONS -----	31
6.	FAIRING LOCATIONS, CENTERLINE, ONE-HALF OFFSET, FULL OFFSET -----	32
7.	FAIRING ATTACHMENT PLATE -----	33
8.	BASELINE TURRET PRESSURE DISTRIBUTION WITHOUT SUCTION -----	34
9.	PRESSURE DISTRIBUTION WITHOUT FUSELAGE SUCTION; FAIRING CENTERLINE -----	35
10.	PRESSURE DISTRIBUTION WITHOUT FUSELAGE SUCTION; FAIRING SUCTION ONE-HALF OFFSET -----	36
11.	PRESSURE DISTRIBUTION WITHOUT FUSELAGE SUCTION; FAIRING FULL OFFSET -----	37
12.	PRESSURE DISTRIBUTION FORWARD FUSELAGE SUCTION; FAIRING CENTERLINE -----	38
13.	PRESSURE DISTRIBUTION FORWARD FUSELAGE SUCTION; FAIRING ONE-HALF OFFSET -----	39
14.	PRESSURE DISTRIBUTION FORWARD FUSELAGE SUCTION; FAIRING FULL OFFSET -----	40
15.	PRESSURE DISTRIBUTION AFT FUSELAGE SUCTION; FAIRING CENTERLINE -----	41
16.	PRESSURE DISTRIBUTION AFT FUSELAGE SUCTION; FAIRING ONE-HALF OFFSET -----	42
17.	PRESSURE DISTRIBUTION AFT FUSELAGE SUCTION; FAIRING FULL OFFSET -----	43

18.	PRESSURE DISTRIBUTION SIDE FUSELAGE SUCTION; FAIRING CENTERLINE -----	44
19.	PRESSURE DISTRIBUTION SIDE FUSELAGE SUCTION; FAIRING ONE-HALF OFFSET -----	45
20.	PRESSURE DISTRIBUTION SIDE FUSELAGE SUCTION; FAIRING FULL OFFSET -----	46
21.	COMBINATION SPHERICAL AND CYLINDRICAL PRESSURE DISTRIBUTION, WITHOUT FUSELAGE SUCTION; ONSIDE IN DIRECTION OF OFFSET -----	47
22.	COMBINATION SPHERICAL AND CYLINDRICAL PRESSURE DISTRIBUTION, SIDE FUSELAGE SUCTION, ON SIDE IN DIRECTION OF OFFSET -----	48
23.	COMBINATION SPHERICAL AND CYLINDRICAL PRESSURE DISTRIBUTION, FUSELAGE SUCTION FORWARD, ON SIDE IN DIRECTION OF OFFSET -----	49
24.	COMBINATION SPHERICAL AND CYLINDRICAL PRESSURE DISTRIBUTION, FUSELAGE SUCTION AFT, ON SIDE IN DIRECTION OF OFFSET -----	50

ACKNOWLEDGMENTS

I would like to express my appreciation to Captain Richard de Jonckheere, U.S.A.F., and the Air Force Weapons Laboratories for providing the funding which afforded the opportunity to conduct this research project.

The excellent technical support provided by Bob Bessel and Ted Dutton, Supervisory Aerospace Engineering Technicians at the Naval Postgraduate School, played an integral part in the wind tunnel experiments and data acquisition. The exquisite, timely, work of Ronald Ramaker in the building of the fairing device was essential to the successful completion of the project.

Lastly, my greatest appreciation for the technical expertise of Dr. Allen E. Fuhs, my thesis advisor, without whose patient guidance this project surely could not have been completed.

I. INTRODUCTION

A. BACKGROUND

The high subsonic flowfield around a laser turret has been the subject of considerable research [Refs. 1,2]. The Air Force Weapons Lab at Kirtland Air Force Base, New Mexico, has instituted much of the research in the study of turbulent flow about a laser turret and how it relates to the optical quality of a high energy laser system currently installed on the NKC-135 aircraft. Several wind tunnel tests have been conducted at NASA Ames 14-foot wind tunnel and have been the subject of four thesis projects at the Naval Postgraduate School 5 x 5 foot wind tunnel [Refs. 3-6].

A high energy laser system focuses large amounts of radiant thermal energy in a small area to destroy targets. When the beam is subjected to jitter or optical distortions, a longer time on target is required to achieve the desired destructive results. To insure that the high energy laser (HEL) is part of our future weapons systems, certain aerodynamic refinements must be made to enhance its effectiveness. The major challenge of this investigation is to attempt to solve the unsteady flow in the aft hemisphere of the laser turret. The density fluctuations due to unsteady flow degrade the optical quality of the laser beam due to propagation through the turbulent medium [Refs. 7,8]. This degradation in the aft hemisphere is due primarily to unsteady flow resulting from

boundary and shear layers as well as vortex shedding. Adaptive optics cannot fully correct the problem so an aerodynamic modification must be obtained. The unsteady pressure loading on the turret also causes jitter which spreads the laser beam and requires longer time on target to achieve the same destructive results as under more stable conditions [Ref. 1].

Several alternatives are available to reduce the thickness and density fluctuations of the turbulent region in the aft hemisphere, thus improving laser propagation. A common boundary layer control method on bluff bodies is accomplished with the addition of surface roughness elements. This promotes early transition to turbulent boundary flow, and the higher momentum turbulent layer separates at a location further along the boundary. However, use of roughness is limited to flows in which the separation is originally laminar. Aircraft turrets operate at high Reynolds Number which results in typically high turbulence, and, therefore, the addition of roughness is clearly not applicable to the turret situation [Ref. 1]. The blowing of air along the surface can reenergize the boundary layer and maintain attached flow. Slot blowing does not appear to be a valid consideration because of the complexity of piping within the turret required to support such a design consideration [Refs. 1,9]. Tangential blowing is particularly attractive due to availability of air from the engine [Ref. 9]. However, this would entail considerable structural modification to the turret itself.

Suction techniques on the turret base and/or on the fairing aft of the turret may also be applied to prevent flow separation and will be the method employed for this study.

In 1980 Schonberger and Mandigo [Refs. 3,4] embarked on a joint thesis study at the Naval Postgraduate School. Testing of a one-third scale model of the turret fairing currently employed on the NKC-135 aircraft was conducted; each researcher designed a fairing nosepiece. Flow control was established by the use of a fuselage boundary layer suction and suction from the fairing aft of the turret. Their findings indicate that quiescent attached flow could be obtained 150° either side of the turret housing, thus increasing the rearward look angle. In 1981, Ripple [Ref. 5] conducted extensive wind tunnel experiments using the Mandigo and Schonberger fairings in the NPS wind tunnel. The results indicate that the previous methods were viable for low velocity, incompressible airflow. He also identified the minimum suction required to achieve the desired results at various parameter combinations. Also, in 1981 Burd [Ref. 6] developed a two-dimensional computer model to design a fairing to investigate flow control by the stabilization of shed vortices with air suction [Ref. 9]. Experimental research using this design was conducted in wind tunnel tests at NPS. Results indicated improved flow performance, but total quiescent flow was not achieved; the experiment was not successful.

B. THESIS OBJECTIVE

The primary objective of this thesis is to design a fairing and suction device necessary to provide quiescent air flow around the laser turret thereby minimizing optical path distortion and jitter. The design should improve the rearward look angle in both azimuth and elevation relative to that demonstrated by Schonberger, Mandigo, and Ripple [Refs. 3-5]. The performance of a mobile fairing was also investigated.

II. FLOW CONTROL

A. THEORY

For two-dimensional flow the pressure coefficients for a sphere and cylinder [Refs. 10,11] are defined as:

$$C_p \text{ (Cylinder)} = \frac{P - P_\infty}{q} = 1 - 4 \sin^2 \theta \quad (1)$$

$$C_p \text{ (Sphere)} = \frac{P - P_\infty}{q} = 1 - \frac{9}{4} \sin^2 \theta \quad (2)$$

where P is the local static pressure on the surface of the body, P_∞ is free stream static pressure, $q = \rho V_\infty^2 / 2$ or free stream dynamic pressure, V_∞ is free stream velocity, ρ is density of the air, and θ the angular distance measured from the forwardmost stagnation point on the turret [Fig. 1].

The geometry of a laser turret can be represented by a hemisphere atop a finite cylinder. The interaction of these geometrical shapes renders a three-dimensional flow, thus giving a C_p value somewhere between the two theoretical values. The diagram for theoretical pressure distribution over any meridian section of a sphere is given in Figure 2 where θ is the angle measured from the forward stagnation point. The theoretical pressure distribution of a cylinder is also contained in Figure 2 giving similar results [Refs. 10,11]. The favorable pressure gradient forward of 90° and 270° maintains attached flow. Aft of the 90° and 270°

points, the pressure gradient is positive in the flow direction resulting in the flow separation which severely degrades laser beam propagation. The essence of this research project is to achieve quiescent flow aft of the 90/270 degree points, as far as possible, thus enhancing laser use in tactical environment.

B. DISCUSSION OF PRESSURE COEFFICIENT

The maximum value for $|C_p|_M$ is obtained when P is zero. Equation (1) can be rewritten as

$$|C_p|_M = \frac{2}{\gamma M_\infty^2} \quad (3)$$

where γ is the ratio of specific heat capacities, and M_∞ is free stream Mach number.

For the experiments reported in this thesis, $M_\infty = 0.03$. Consequently, $|C_p|_M$ has a value of approximately 1600. For flight at $M = 0.6$, the value of $|C_p|_M$ is approximately 4.

Due to the low Mach number a very large value of C_p can be obtained. Typically one expects $|C_p|$ is less than 10, but in subsequent figures values of $|C_p|$ as large as -61.8 will be found. The reader should be alerted that the large value of $|C_p|$ is not abnormal compared to $|C_p|_M$.

For flight at higher Mach numbers, the suction technique may not be useful due to aerodynamic choking in the gap area. Tests at flight Mach numbers should be conducted.

C. METHOD OF FLOW CONTROL

There are several methods of controlling separated air flow about aircraft turrets [Refs. 8,9]. The method selected for this research project incorporates suction at the base of the turret and through a fairing located aft of the turret, as shown in Figure 3. The suction will maintain attached flow around the turret.

III. EXPERIMENTAL APPARATUS

A. PHYSICAL COMPONENTS

The primary components, with the exception of the fairing device and nosepieces, were unchanged from previous experiments and are described in detail in References 1, 2, and 3. The components consisted of the Naval Postgraduate School 5 x 5 foot wind tunnel where a one-third scale model turret and fairing device were located. An Aerovent centrifugal blower and drive motor assembly were mounted underneath the wind tunnel and connected via a six-section duct housing to the floor of the wind tunnel. This provided the required suction for the fairing and fuselage bleed slot.

Perforated sheeting, as described in Reference 3, was installed on the fuselage bleed slot simulating a porous condition. The propeller anemometers, also from Reference 3, were employed to measure suction duct velocities, but the locations were changed and renumbered to accommodate the smaller fairing device (Fig. 3).

New base plates were manufactured from wood to accommodate the turret. Because of the dimensions of the plenum chamber, two base plates were required for the trials simulating fuselage suction, one for the base plate fore and aft and one for side suction (Fig. 4). A series of three runs was also made with a solid base plate without fuselage bleed suction.

The fairing device is significantly smaller than previously tested (Fig. 5). The fairing is hollow and has no nosepiece,

which required some modification of the ducting from prior experiments. For most test runs the fairing used only the forwardmost duct. Two suction ducts were required for one configuration because of the dimensions of the plenum and will be discussed further in Section IV.A.

B. INSTRUMENTATION

Forty-eight pressure taps are installed in the turret and wind tunnel to facilitate pressure distribution measurement for the turret. Pressure tap locations for the turret can be found in Figure 1. The forty-eight pressure taps are connected to a scanivalve pressure transducer by flexible Tygon plastic tubing. Locations of the taps with respect to the scanivalve are given in Table I. The voltage sensed by the scanivalve is sent to the INTEL 80/10 computer where a digital readout may be obtained. A control program was developed which enabled the voltages to be printed by an AN/UGC-59A teletypewriter. A calibration procedure was developed [Refs. 3,4] which provided a linear relationship between voltage and pressure. This relationship was used to calculate pressure coefficients and wind tunnel velocity. Appendix A contains an example of the formulas used in these calculations.

Anemometer voltage readings were recorded via a digital multimeter and oscilloscope. The second degree equations for converting duct velocity as a function of voltage can be found in Appendix A.

Additional yarn tufts were added to the turret and fairing device to visualize the flow condition.

IV. EXPERIMENTAL RESULTS

A. TEST PROCEDURE

Twelve separate test conditions were examined in this project. The test conditions will now be described.

1. Fairing Suction Device

The fairing device had three separate configurations relative to the turret housing. They were centerline, one-half offset and full offset (Fig. 6). When the fairing was offset, a side plate of variable length was attached to obtain laminar flow with minimum suction on the side opposite the fuselage bleed slot (Fig. 7). Tufts were added to the far side of the turret, which is normally obscured. A mirror was then mounted on the far wall of the wind tunnel to provide viewing. These variations were examined for the possibility of adapting a small mobile fairing device and the benefits derived in terms of increasing the allowable firing bearings of the laser.

2. Fuselage Bleed Slot

The fuselage bleed slot had four configurations: none, forward, side and aft (Fig. 4). The fairing offset was placed in the opposite direction of the fuselage bleed slot.

3. Measurements

Minimum duct velocity was determined for the fairing and fuselage suction. Turret pressure measurements and wind tunnel velocity data were also recorded. When the fuselage

base suction was placed aft, the fairing device had to be moved aft. When the fairing was moved aft, suction was received from two ducts. The separation distance from the turret to the fairing was much greater for this run which increased the mass flow rate through the fairing substantially. As a result of this increased flow rate, the propeller anemometer was over stressed, and the shaft fractured. Suction duct velocity was not recorded for the three runs in this sequence.

Naturally occurring boundary layer transition was expected around the turret since the value of the Reynolds Number was in the critical range [Refs. 3-6].

Evaluation of the pressure distributions around the turret for spherical, cylindrical and a combination using ports 28, 20, 19, 24, and 32 for spherical across the turret top, 36 through 40 for cylindrical and 28 through 32 at the sphere and turret interphase (Fig. 1), were then plotted as a function of θ for the side away from offset (Figs. 8-20). Pressure distribution for the side in the direction of offset for the combination spherical and cylindrical can be found in Figures (21-24) using ports 28, 35, 34, 33, and 32.

B. RESULTS

The trials were organized into four cases. Figures (8-20) illustrate pressure distributions for the twelve trials and a baseline for the turret without suction. The figures are a plot of C_p as a function of angular position on the turret.

Figure 8 was taken as a baseline, with fairing centerline, and without fuselage or fairing suction which shows an unfavorable pressure gradient aft of 90°. There was a great deal of tuft motion indicating flow separation aft of the 90° point. The C_p for the sphere measurement was higher than that of the cylinder as would be expected. The cylinder did not obtain a C_p of -3 probably as a result of three dimensional flow and the fact that it is not an infinite cylinder (Fig. 2). Figures (9-20) were constructed for each of the twelve separate trials and are also a plot of C_p as a function of angular position on the turret. Due to the configuration of the port locations (Fig. 1) the data points on each figure that were known were at 0°, 45°, 90°, 135°, and 180°.

Gap velocity, V_g , can be defined as the velocity of air between the fairing device and the turret and can be calculated using the formula as follows:

$$V_g = \sum V_d A_d / A_g \quad (4)$$

where V_d is the velocity in the duct, A_d is the area of the duct, and A_g is the area between the turret and the fairing device. The resultant values are incorporated in Figures (8-20) and Table II.

The flow ratio for each case can also be found in Figures (8-20) and Table II. The flow ratio can be defined as volume flow rate into the fairing divided by the volume flow rate

at free stream velocity in the wind tunnel, with cross sectional area equal to the projected laser turret area. This ratio can be represented as,

$$R = \int V_d A_d / V_\infty A_p \quad (5)$$

where V_d is the velocity in the duct, A_d is the area of the duct, V_∞ is free stream velocity and A_p is the projected turret area. V_∞ varied with each configuration, and A_p is 1.89 ft².

1. Case One

Case One consists of the three fairing conditions without fuselage suction (Figs. 9-11). Visually interpreting the tufts for centerline and one-half offset fairing configurations indicated dramatic improvement with respect to the no suction case. The only tuft fluctuations noted just ahead of the fairing on the turret. The full offset configuration remained moderately turbulent. In an attempt to quiet the turbulence, two sizes of angle iron were screwed to the floor of the wind tunnel opposite fairing offset to channel the flow. The larger of the two angle irons increased the turbulence while the smaller one resulted in only a slight improvement. A hole was cut in the fairing base plate opposite the offset. A metal plate was used to vary the suction area, but the configuration was not able to eliminate the turbulence. The pressure distribution for all trials in this

case did show a pressure rise at the 135° point on the turret. For optimum conditions, the suction duct velocities for center-line, one-half offset and full offset were 43.52 ft/sec, 36.74 ft/sec, and 44.33 ft/sec. The one-half offset repeatedly required the least suction of the fairing locations throughout all trials. Figures 10, 13, 16, and 19 are germane.

A silent 16-mm. movie showing tuft motion with and without flow control for this case can be requested on loan from Distinguished Professor Allen E. Fuhs, Code 67 Fu, Department of Aeronautics, United States Naval Postgraduate School, Monterey, California, 93940.

2. Case Two

The configuration consisted of forward fuselage suction and the three fairing locations (Figs. 12-14). Results were similar to that of Case One except less suction velocity was required through the fairing. Turbulent flow for the full offset condition persisted.

3. Case Three

Aft fuselage suction and the three fairing locations comprised these trials (Figs. 15-17). The fairing at center-line was placed three inches away from the turret on the near side and one and one-eighth inches on the far side with the extension plate attached. The increased distance was required due to the two inch fuselage suction slot being aft of the turret. During the first of these runs the propeller anemometer sheared, and suction duct velocity readings were not

obtained. Slight turbulence was observed for all fairing locations; the turbulent region progressed up the body of the turret as the offset increased.

4. Case Four

The three trials in this series consisting of side fuselage suction and the three fairing offsets (Figs. 18-20) produced similar results to those without a fuselage suction (Figs. 9-11). Turbulence was observed on the after portion of the turret when the fairing was full offset. Turbulence was not observed for centerline and one-half offset cases. The pressure distribution plot still indicates a pressure rise at the 135° point of the turret in all cases. Duct velocities for centerline, one-half offset, and full offset were 47.93 ft/sec, 36.12 ft/sec, 48.5 ft/sec and fuselage suction was 15.1 ft/sec, 14.3 ft/sec and 13.69 ft/sec, respectively. The suction duct velocities were in close agreement with those measured without fuselage suction. The velocities were recorded with a new anemometer as a result of the failure in Case Three.

A summary of all trials has been placed in tabular form in Table II.

V. CONCLUSIONS

The concept of using afterbody suction as a means of providing flow control with a geometrically smaller fairing than previously tested [Refs. 3-6] has proven effective for incompressible flow at critical Reynolds Number and low velocity and can be observed in the 16-mm movie obtained on request from Distinguished Professor Fuhs. During all trial conditions, the one-half offset fairing consistently required less suction to stabilize the turret tufts. Further testing to optimize the fairing offset and attachment plate gap should be considered. If an adequate design could be developed for the employment of a moveable fairing, its incorporation would significantly improve laser arcs of fire.

The smaller fairing device is not without penalty. It can be seen from the large flow ratio ranging from 0.36 to 0.54 and gap velocities from 137 ft/sec to 175 ft/sec that a significant amount of suction necessary to maintain quiescent flow would be required. This requirement could be diminished somewhat by the use of fuselage suction.

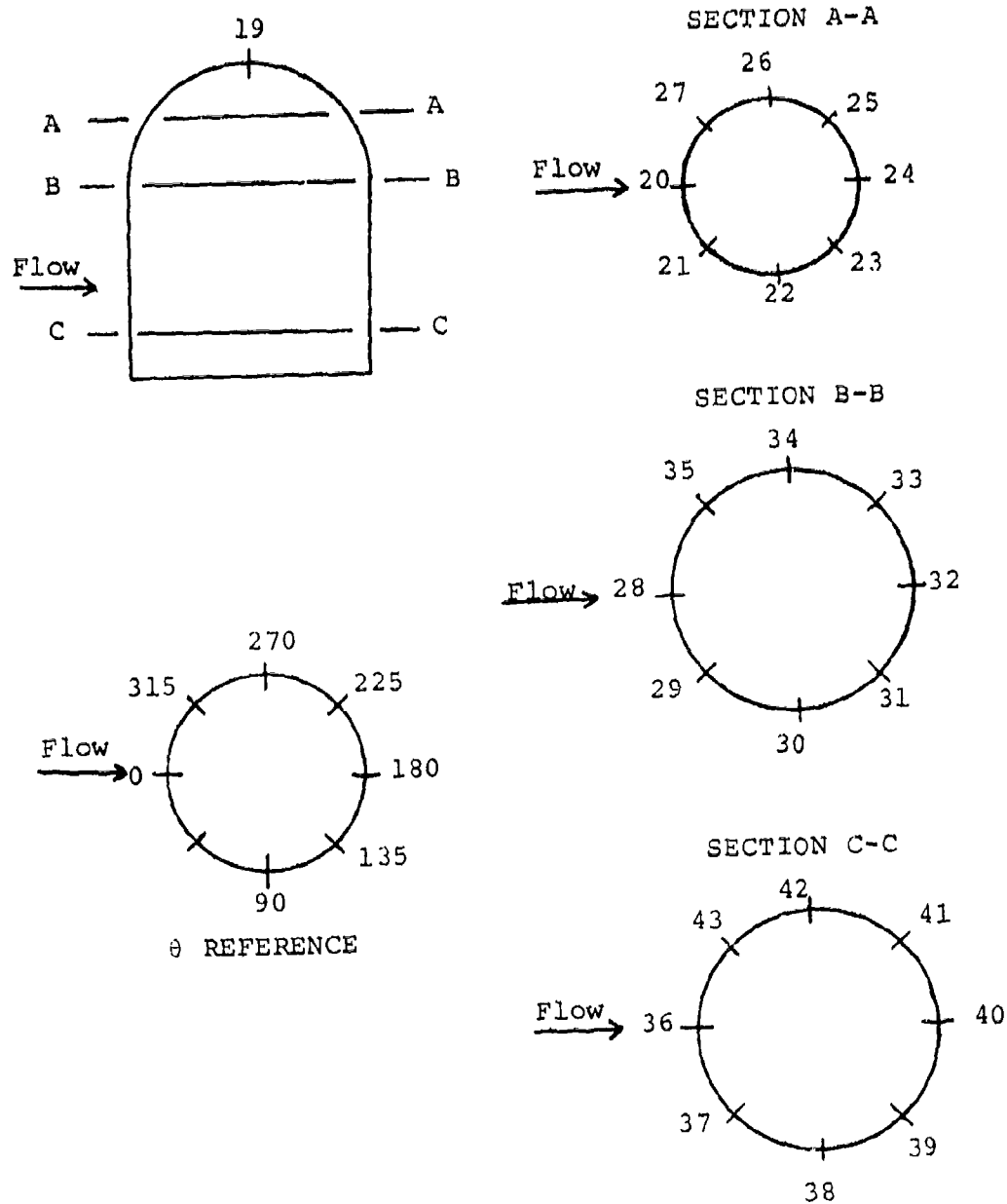


Figure 1. TURRET PRESSURE TAP LOCATIONS

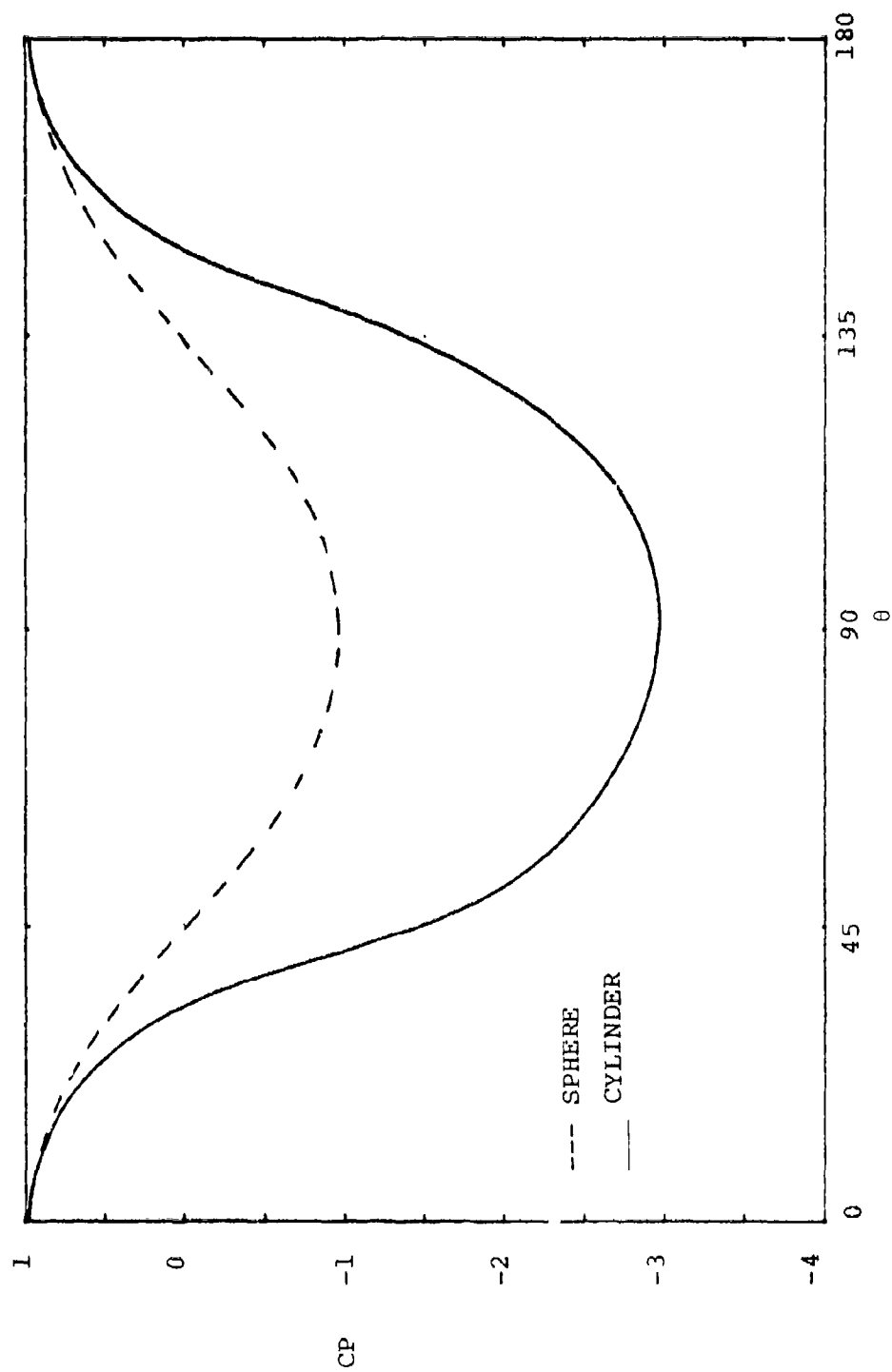


Figure 2. THEORETICAL PRESSURE DISTRIBUTION FOR A
SPHERE AND CYLINDER

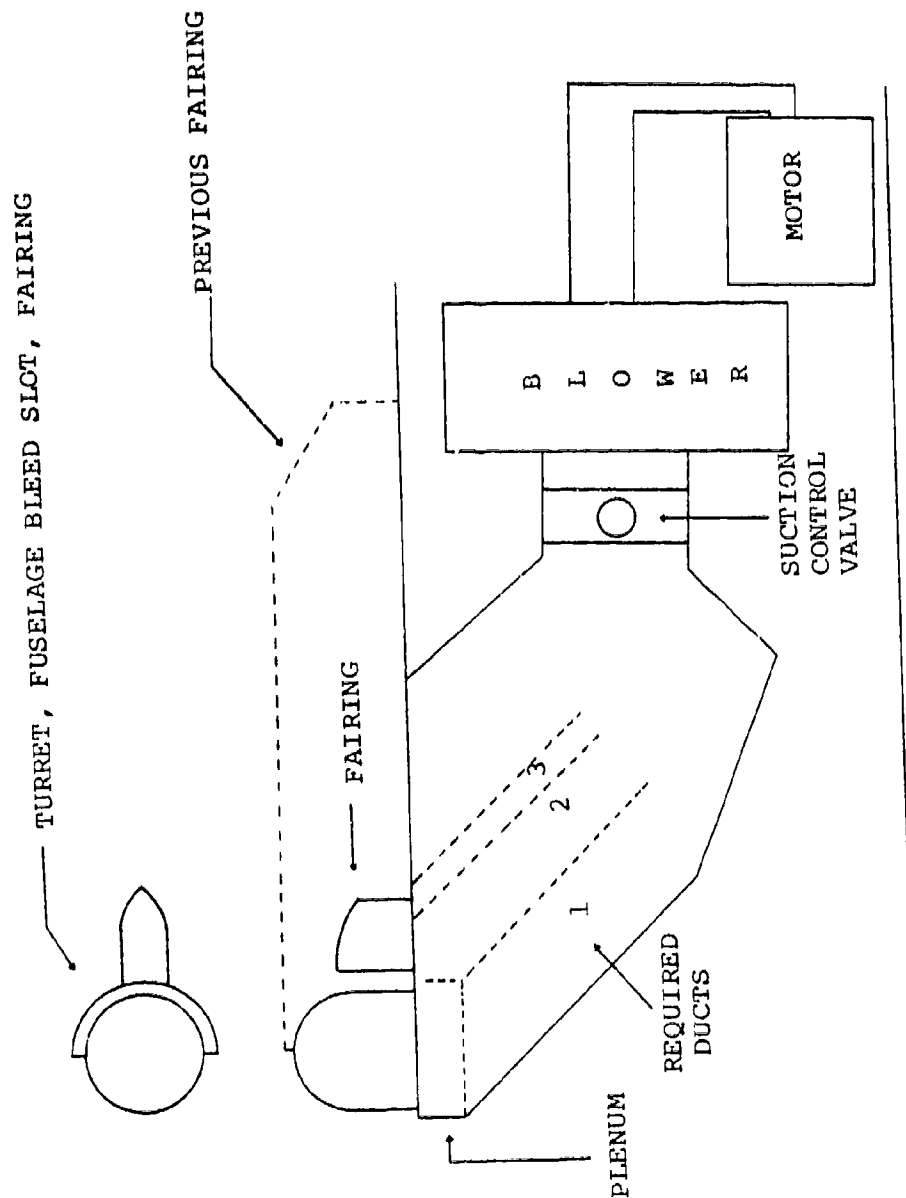


Figure 3. LASER TURRET, FAIRING, AND WIND TUNNEL CONFIGURATION

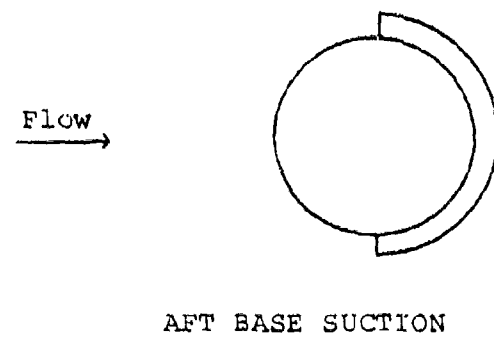
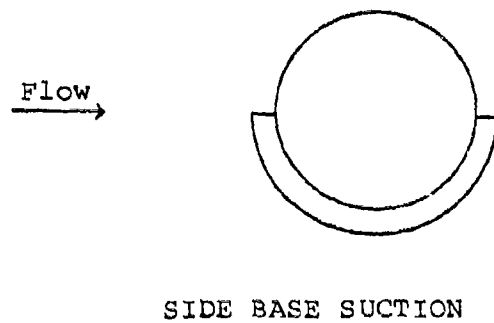
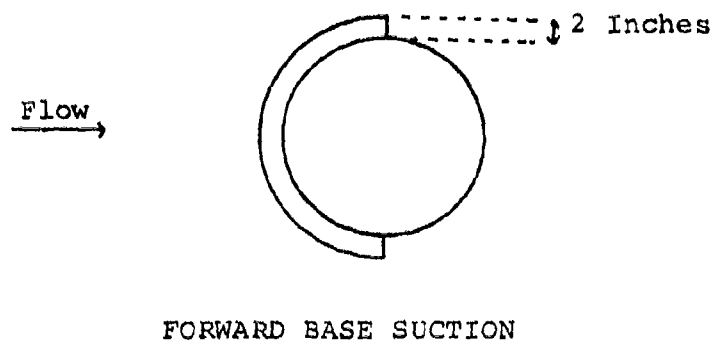


Figure 4. FUSELAGE BLEED SLOT, FORWARD, SIDE, AND AFT

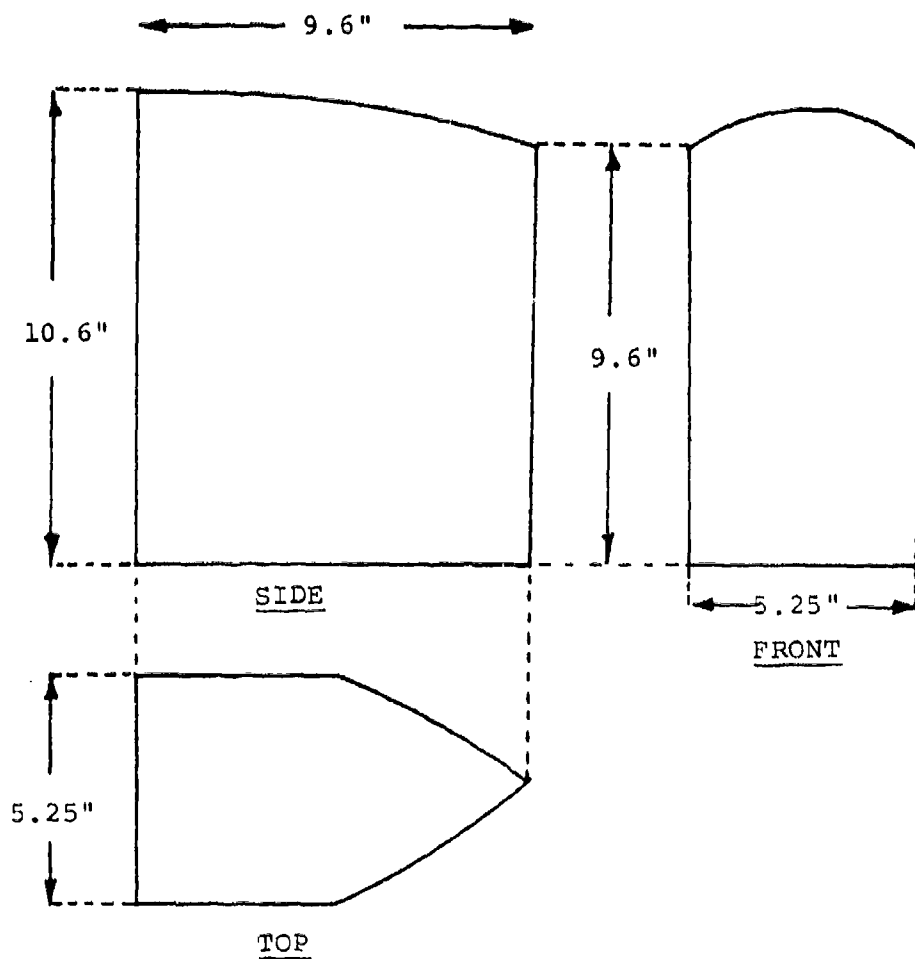


Figure 5. FAIRING DIMENSIONS

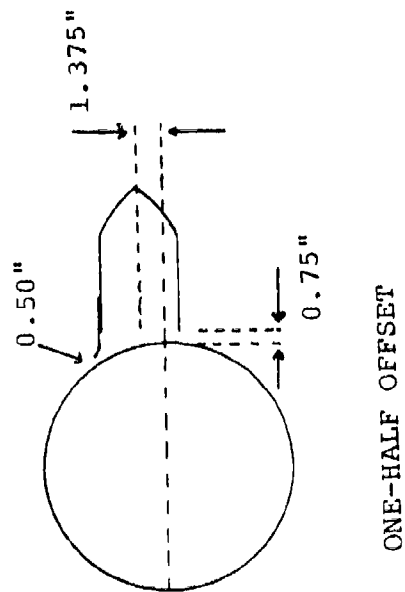
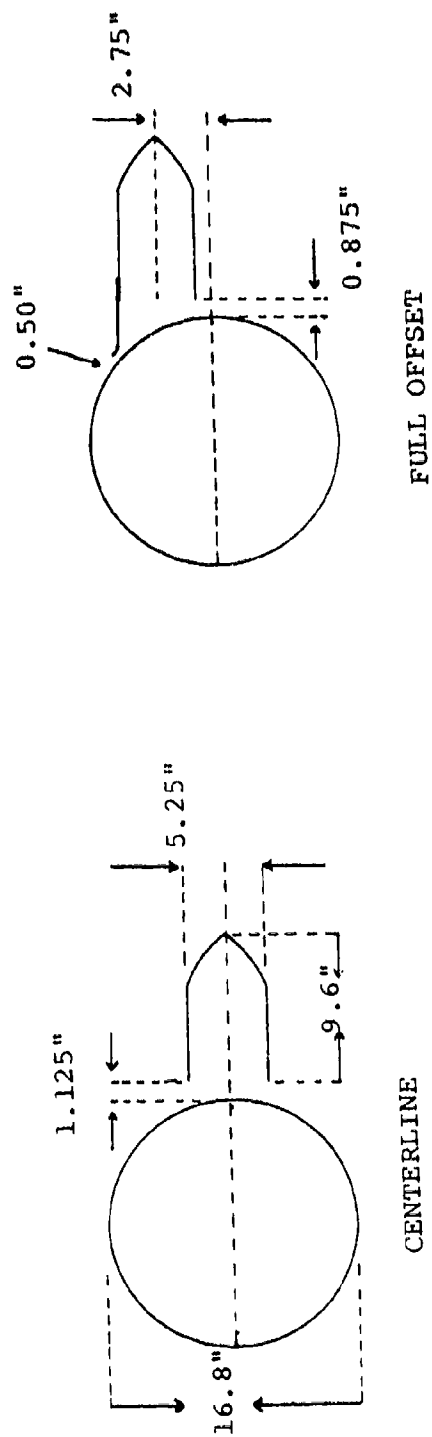


Figure 6. FAIRING LOCATIONS, CENTERLINE, ONE-HALF OFFSET
FULL OFFSET

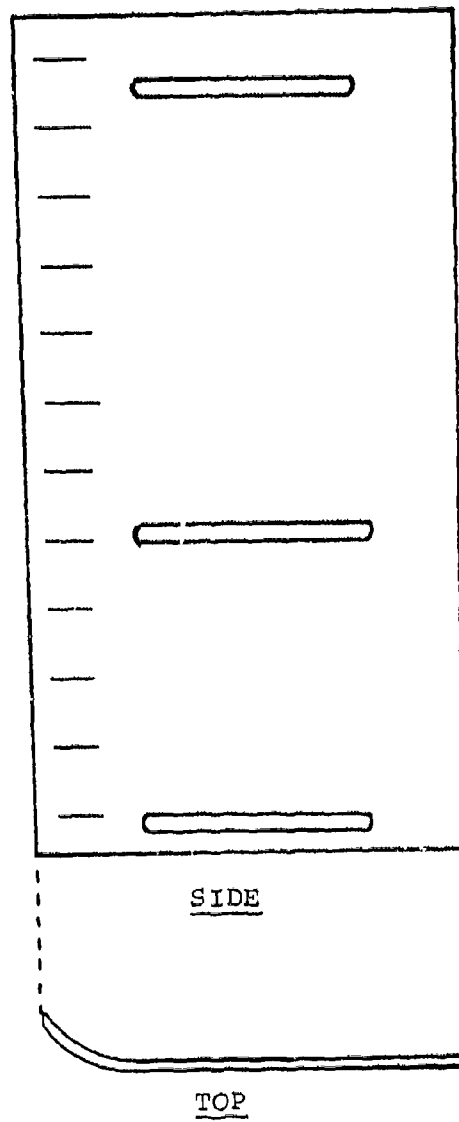


Figure 7. FAIRING ATTACHMENT PLATE

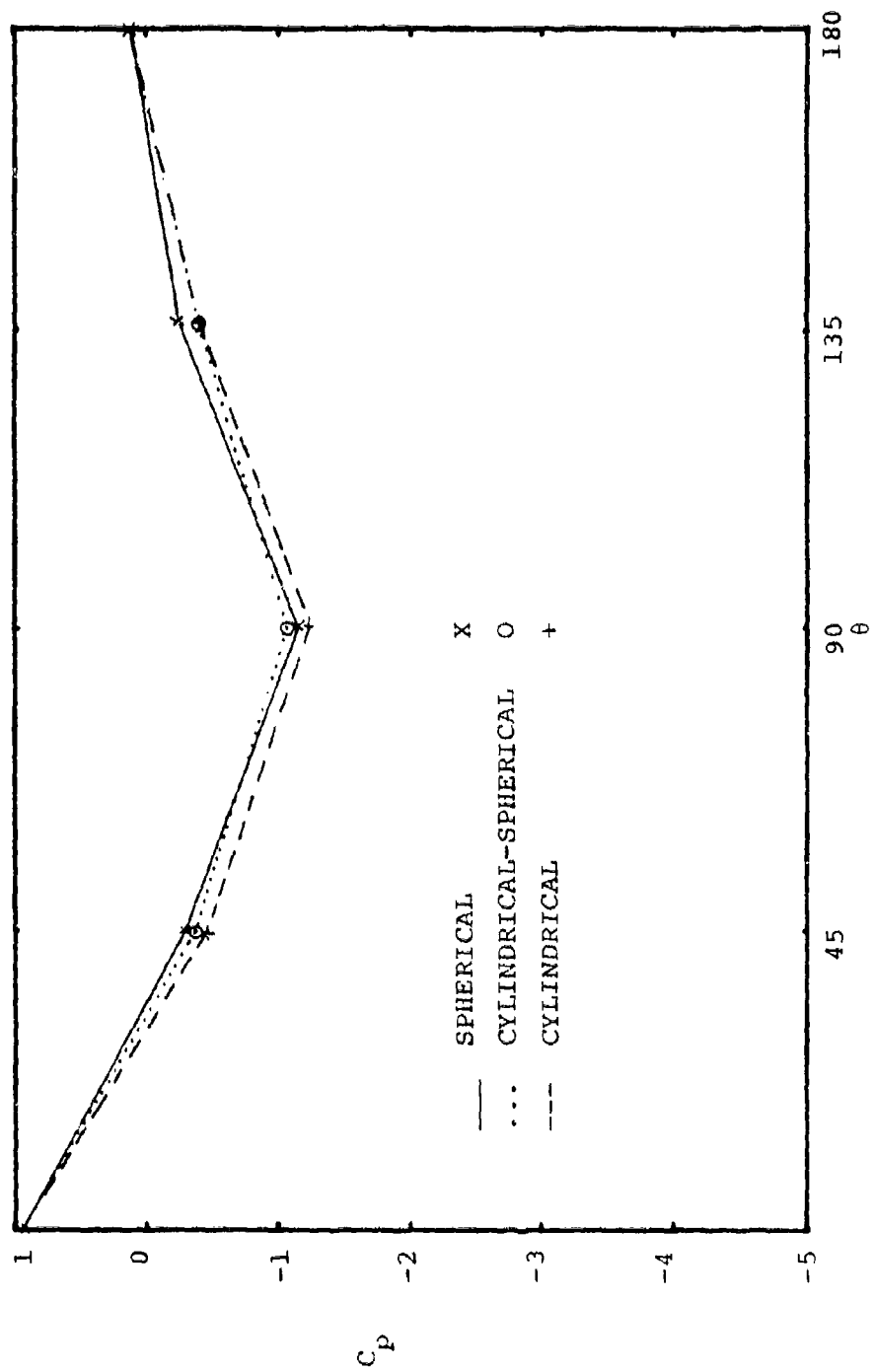


Figure 8. BASELINE TURRET PRESSURE DISTRIBUTION WITHOUT SUCTION

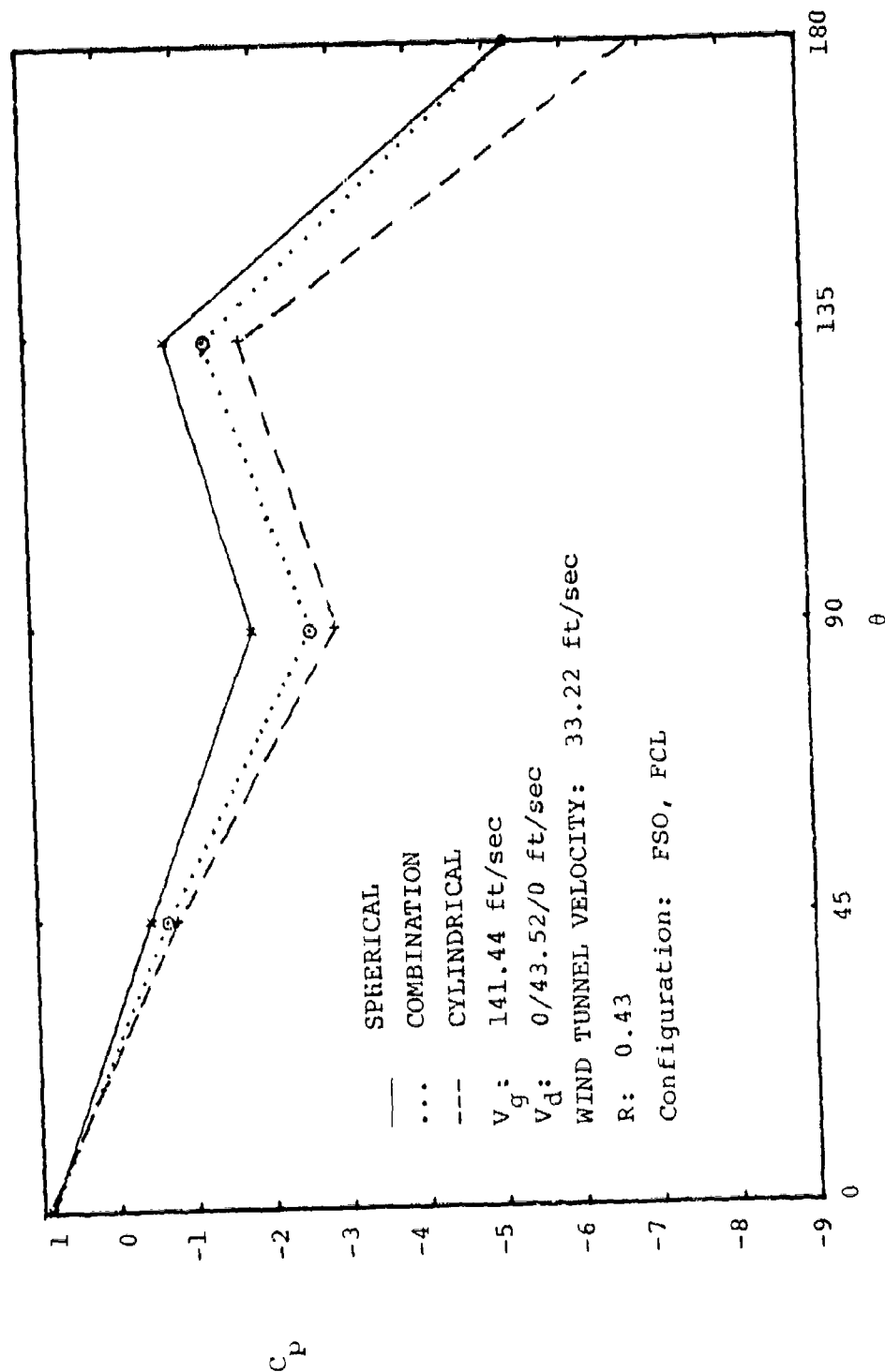


Figure 9. PRESSURE DISTRIBUTION WITHOUT FUSELAGE SUCTION; FAIRING CENTERLINE

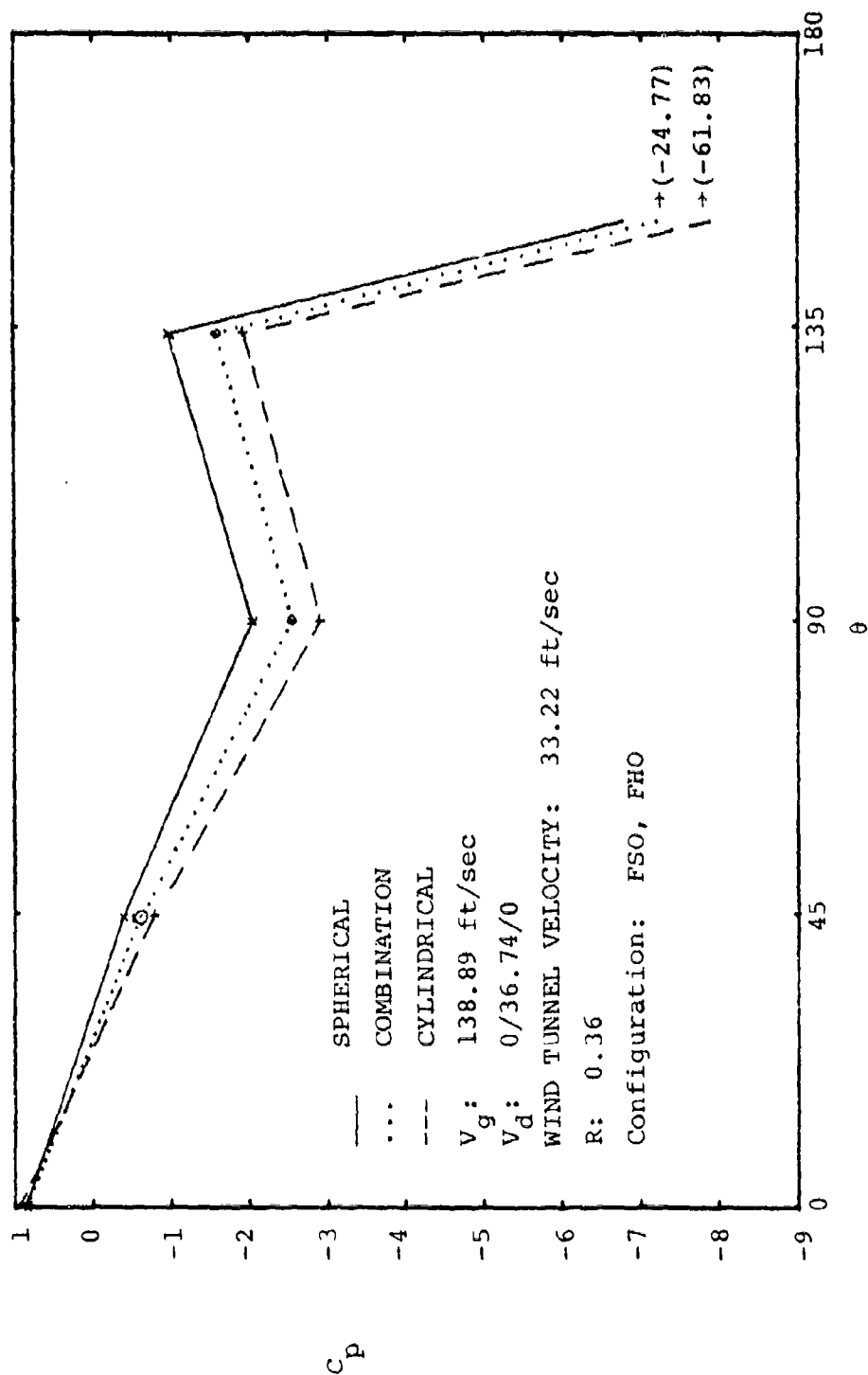


Figure 10. PRESSURE DISTRIBUTION WITHOUT FUSELAGE SUCTION;
FAIRING SUCTION ONE-HALF OFFSET

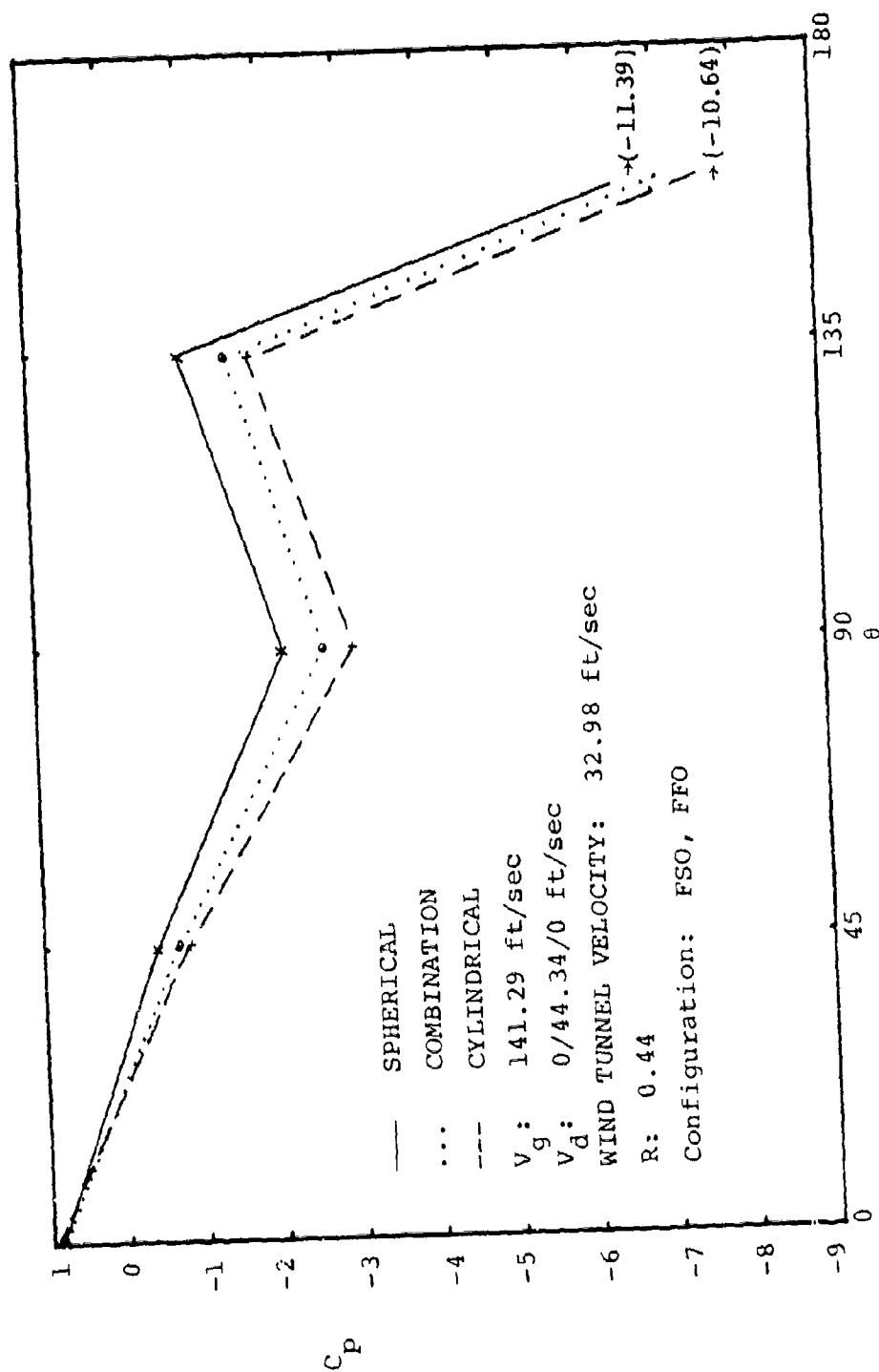


Figure 11. PRESSURE DISTRIBUTION WITHOUT FUSELAGE
SUCTION; FAIRING FULL OFFSET

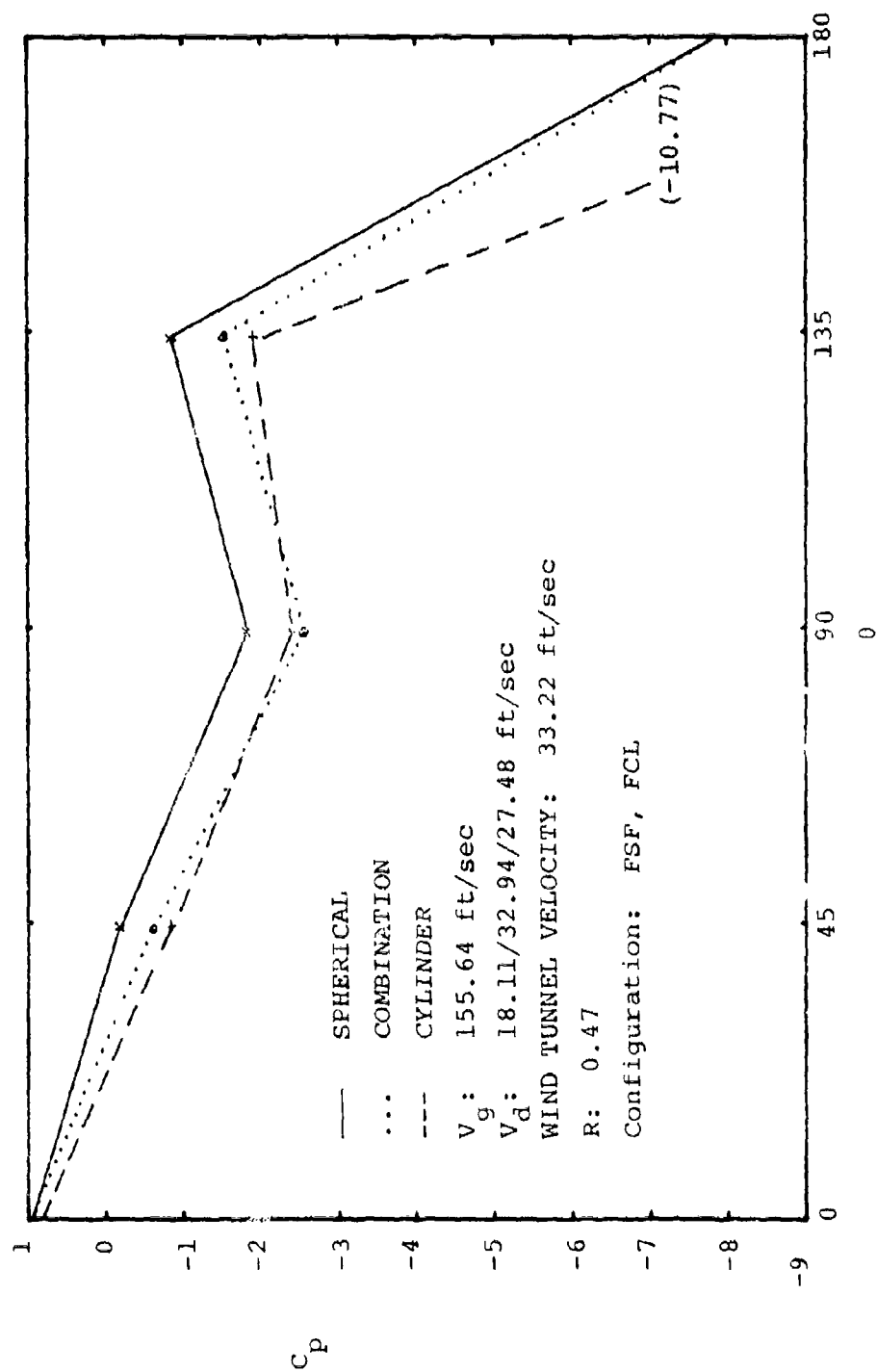


Figure 12. PRESSURE DISTRIBUTION FORWARD FUSELAGE
SUCTION; FAIRING CENTERLINE

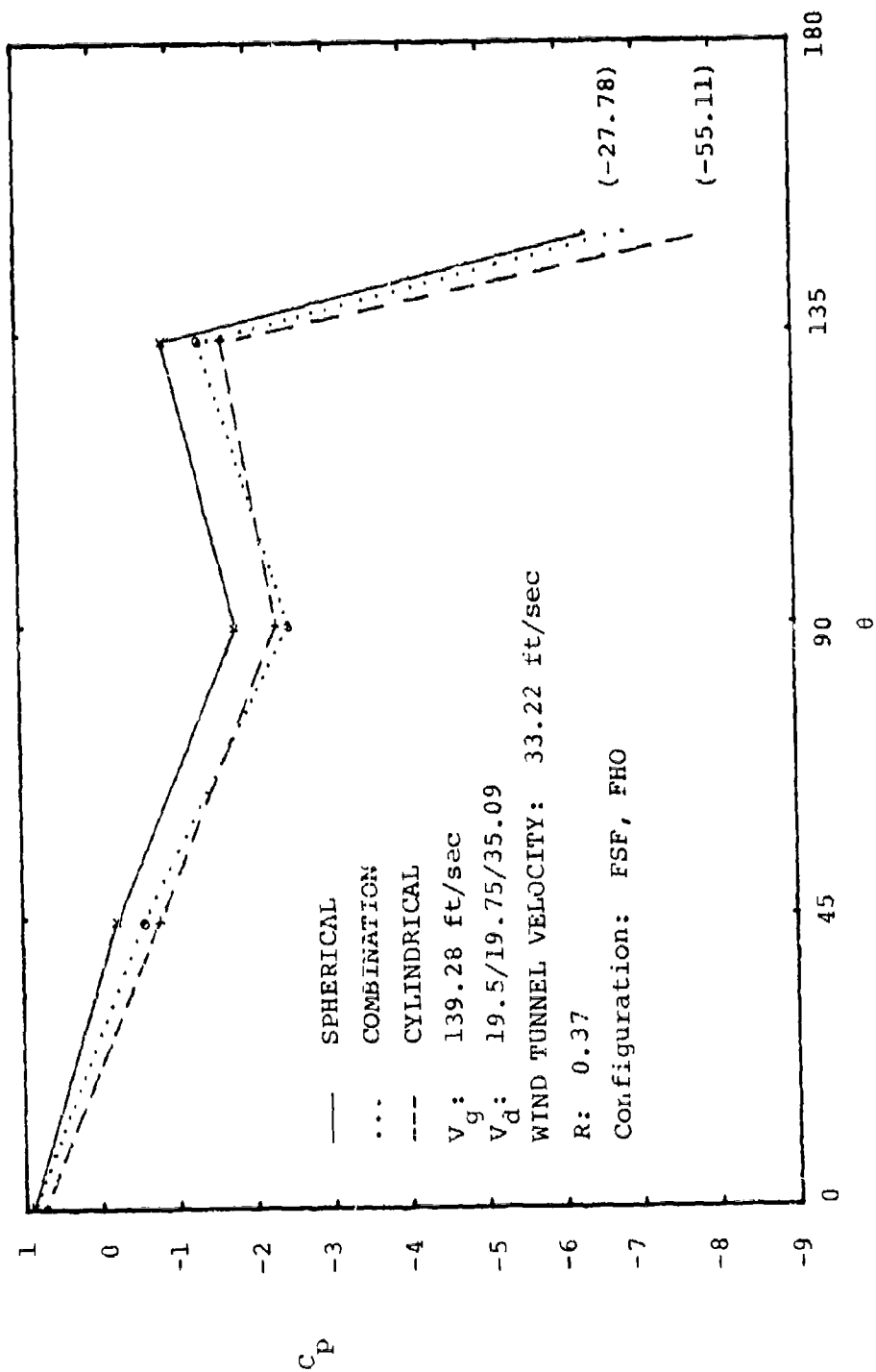


Figure 13. PRESSURE DISTRIBUTION FORWARD FUSELAGE
SUCTION; FAIRING ONE-HALF OFFSET

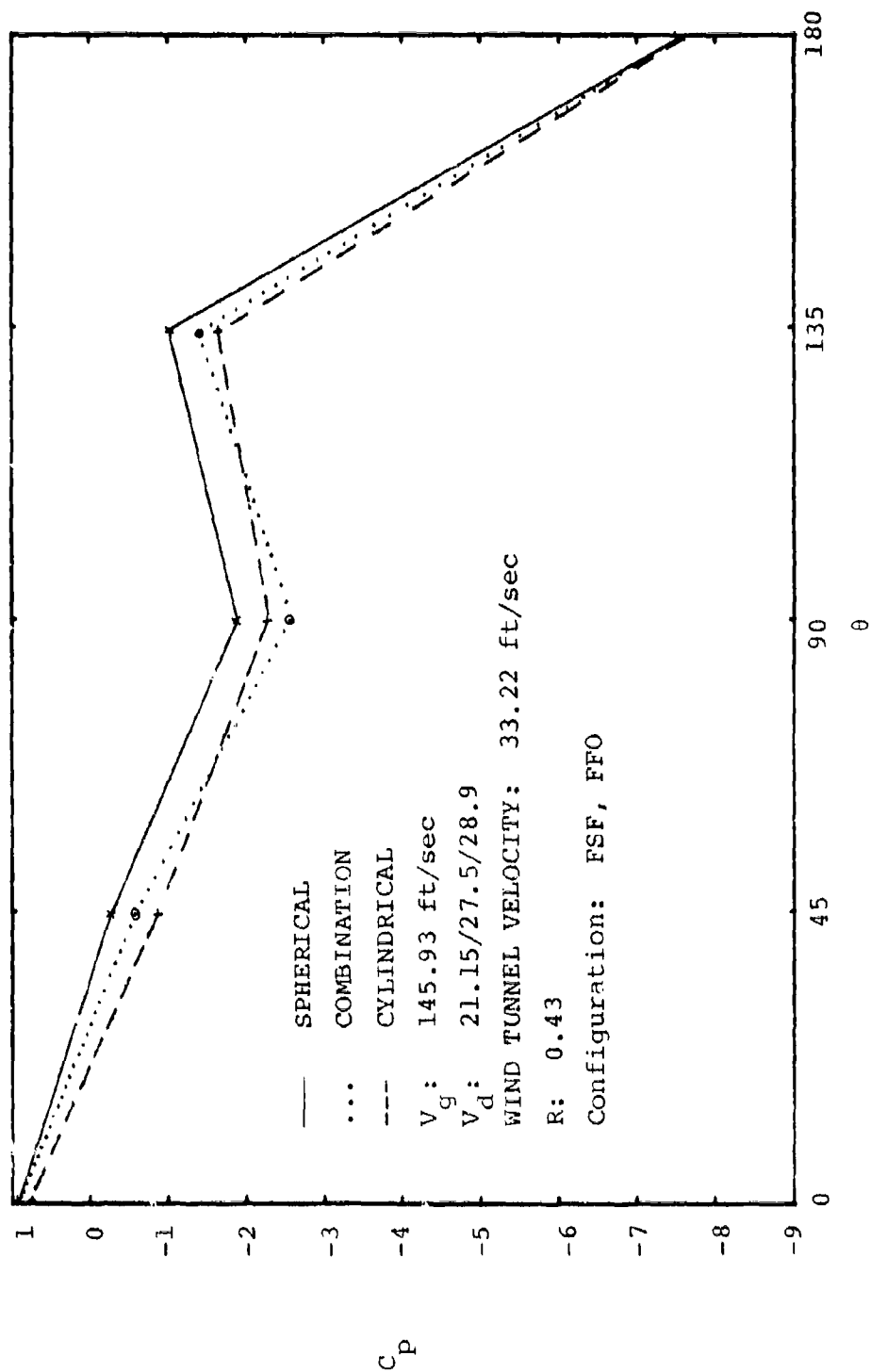


Figure 14. PRESSURE DISTRIBUTION FORWARD FUSELAGE
SUCTION; FAIRING FULL OFFSET

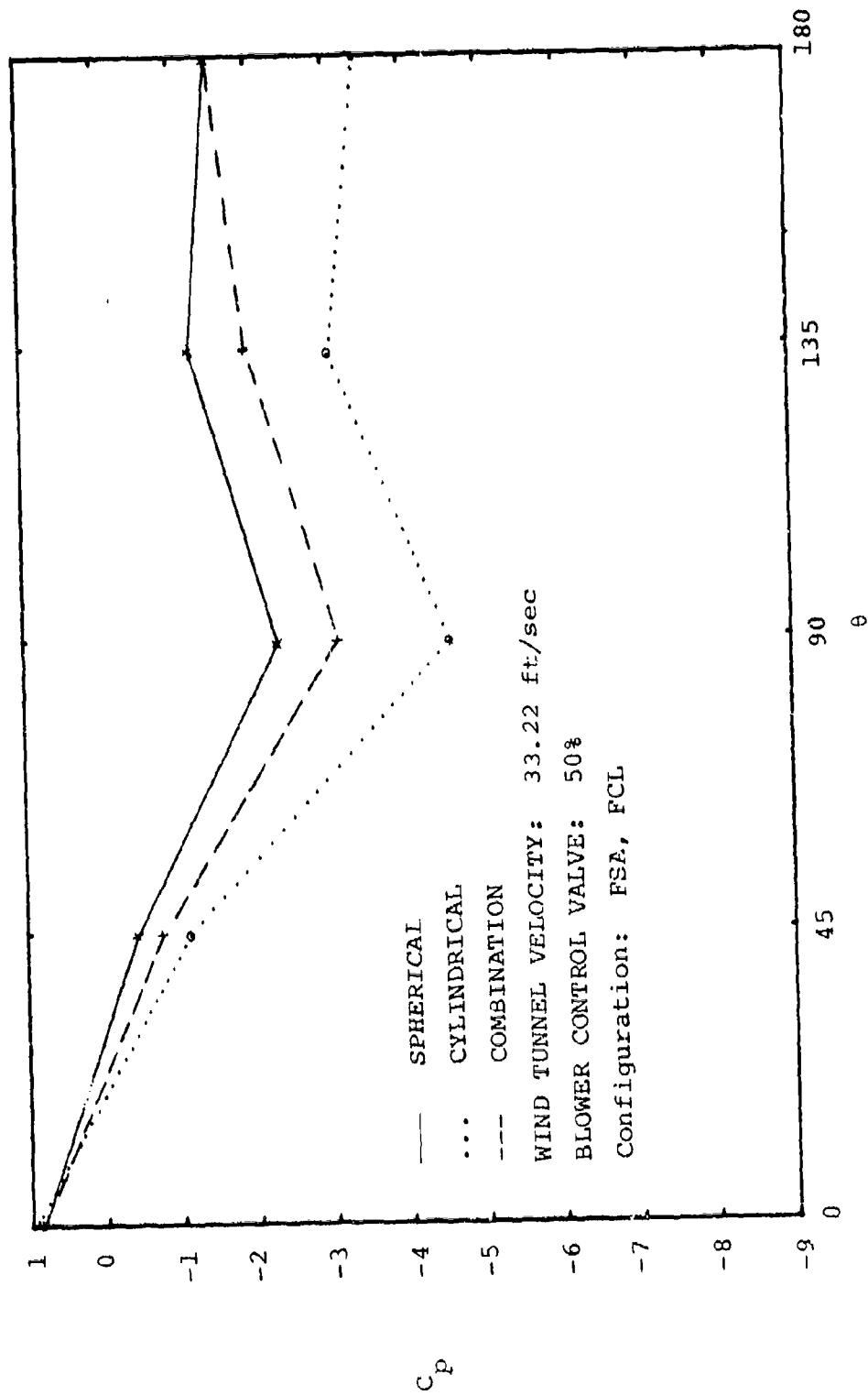


Figure 15. PRESSURE DISTRIBUTION AFT FUSELAGE
SUCTION; FAIRING CENTERLINE

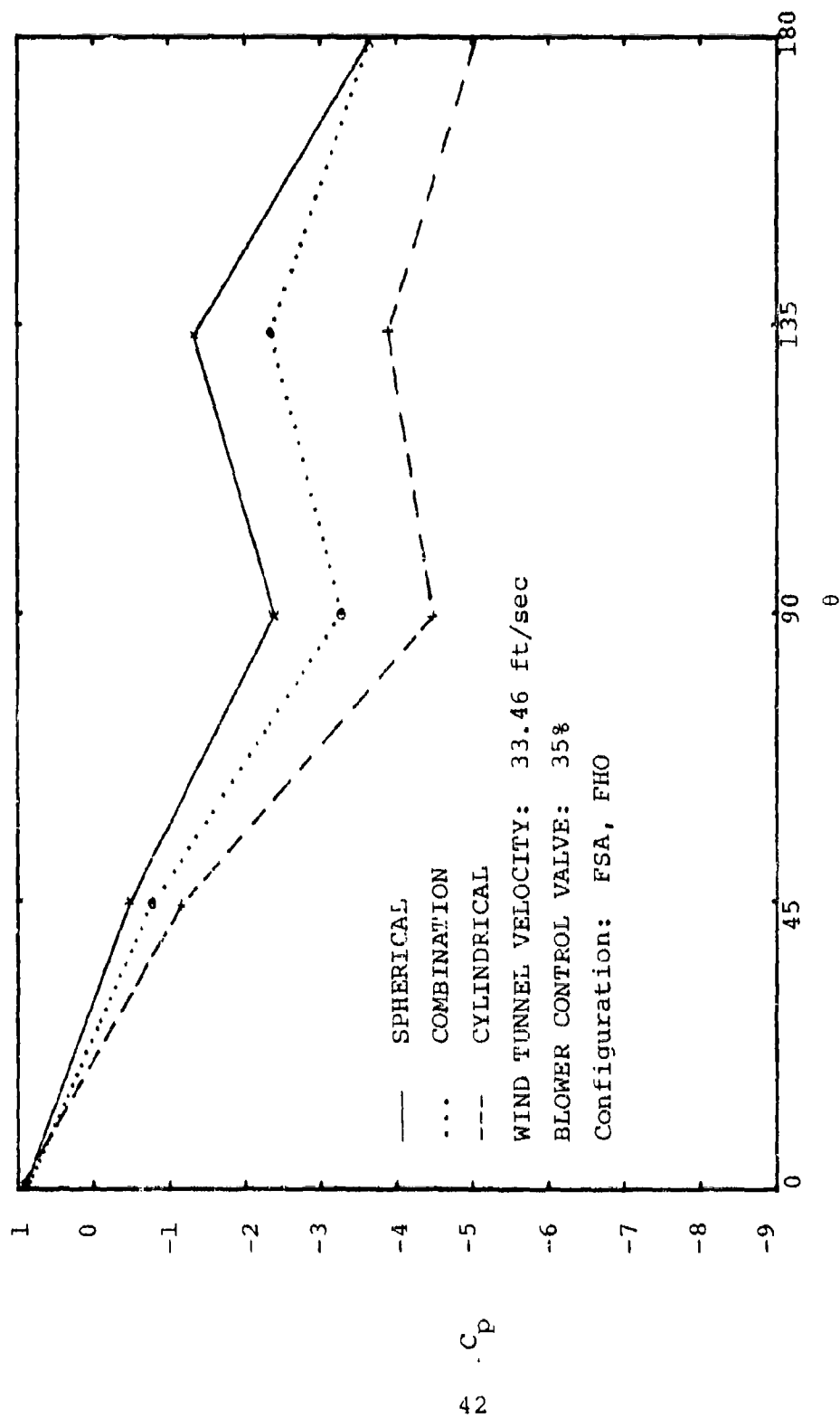


Figure 16. PRESSURE DISTRIBUTION AFT FUSELAGE SUCTION; FAIRING ONE-HALF OFFSET

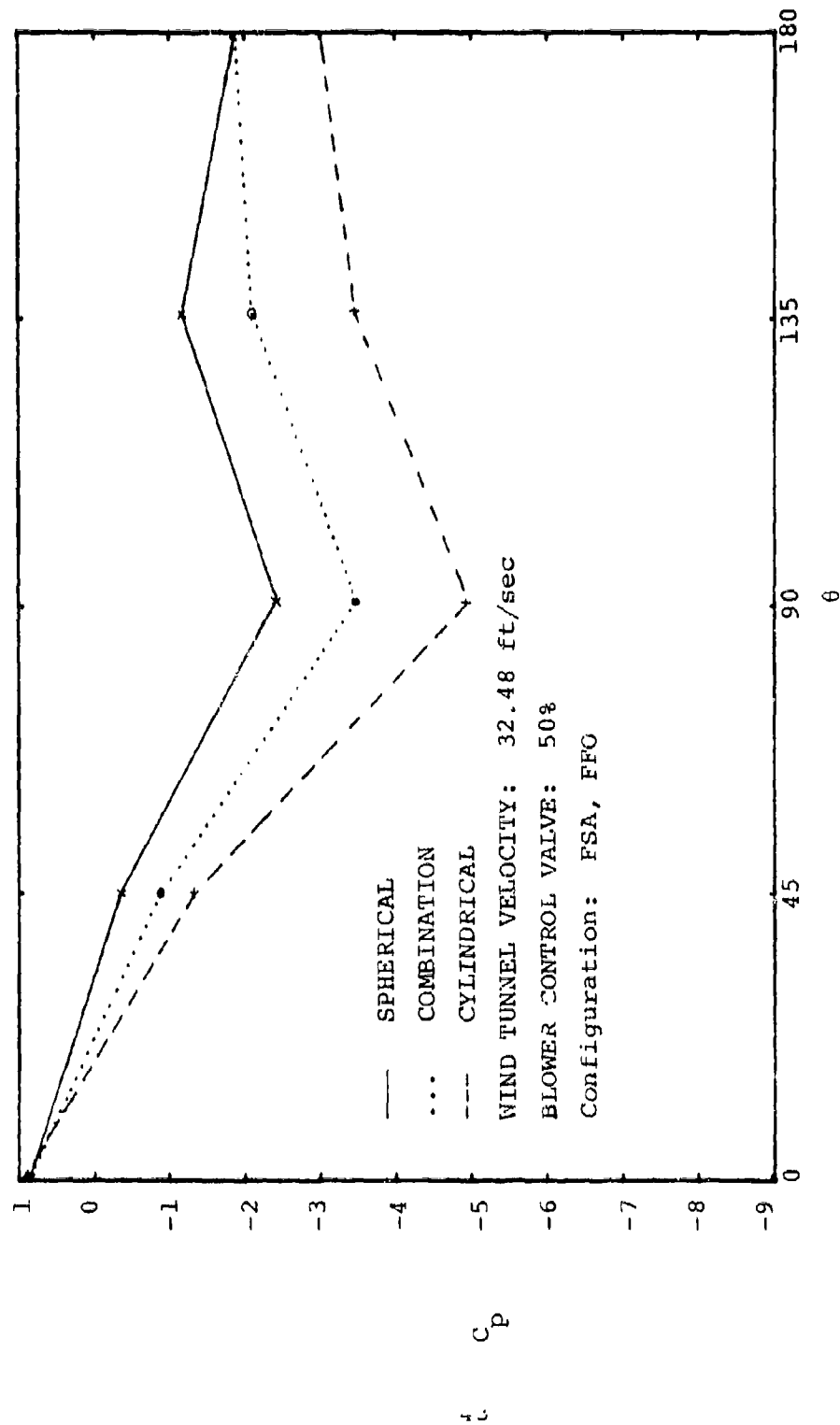


Figure 17. PRESSURE DISTRIBUTION AFT FUSELAGE
SUCTION; PAIRING FULL OFFSET

1
 0
 -1
 -2
 -3
 -4
 -5
 -6
 -7
 -8
 -9

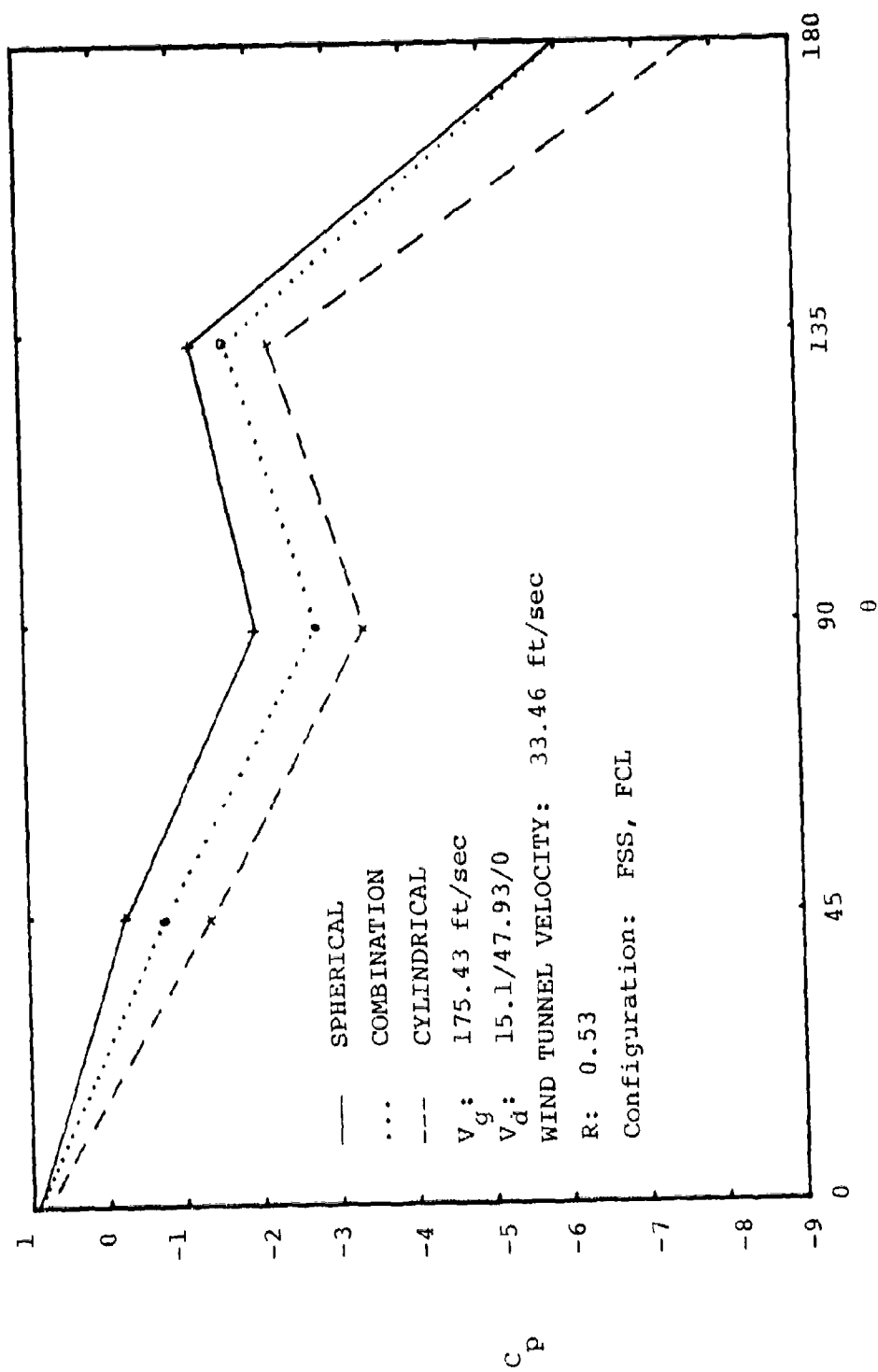


Figure 18. PRESSURE DISTRIBUTION SIDE FUSELAGE
SUCTION; FAIRING CENTERLINE

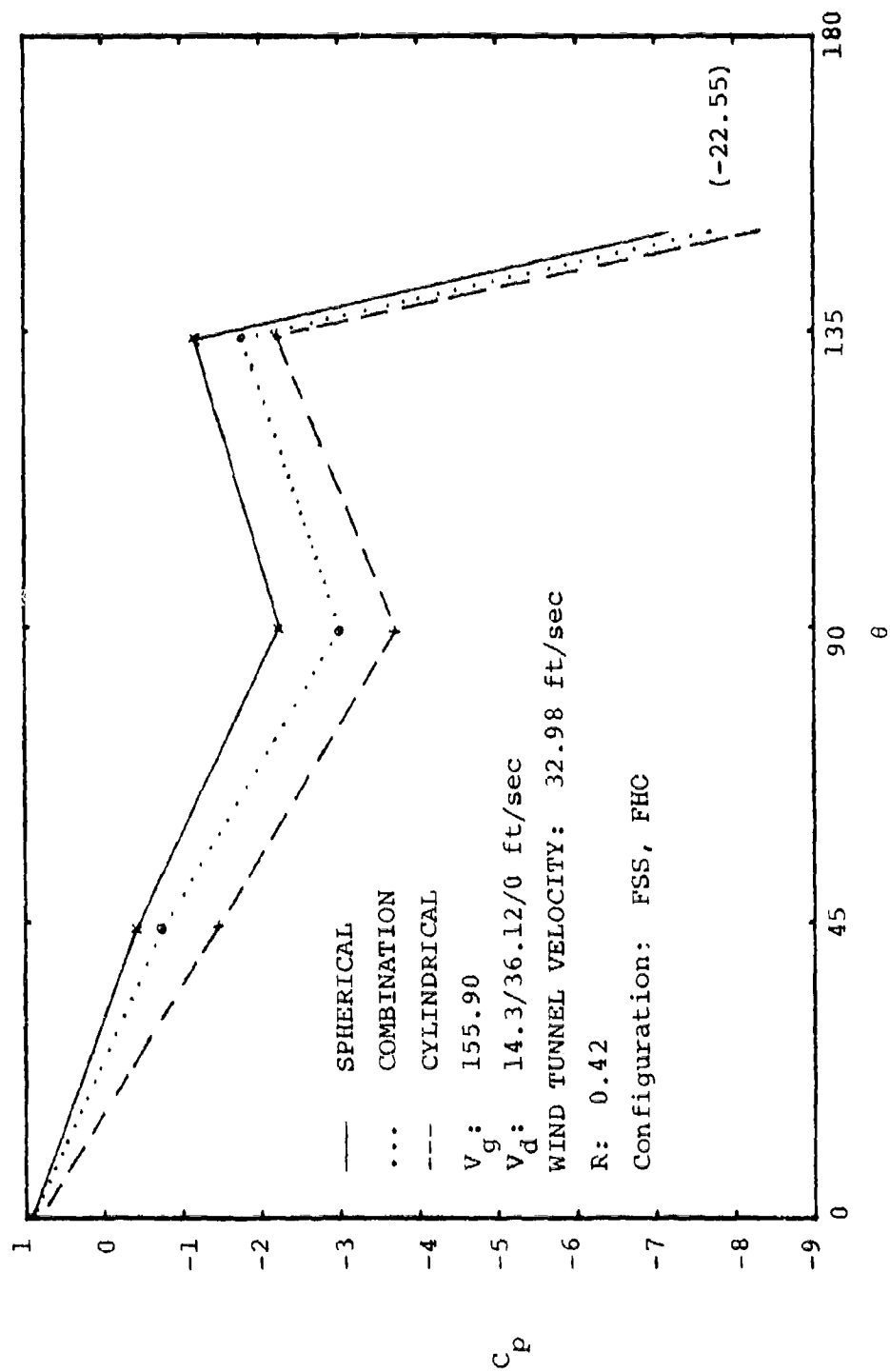


Figure 19. PRESSURE DISTRIBUTION SIDE FUSELAGE
SUCTION; FAIRING ONE-HALF OFFSET

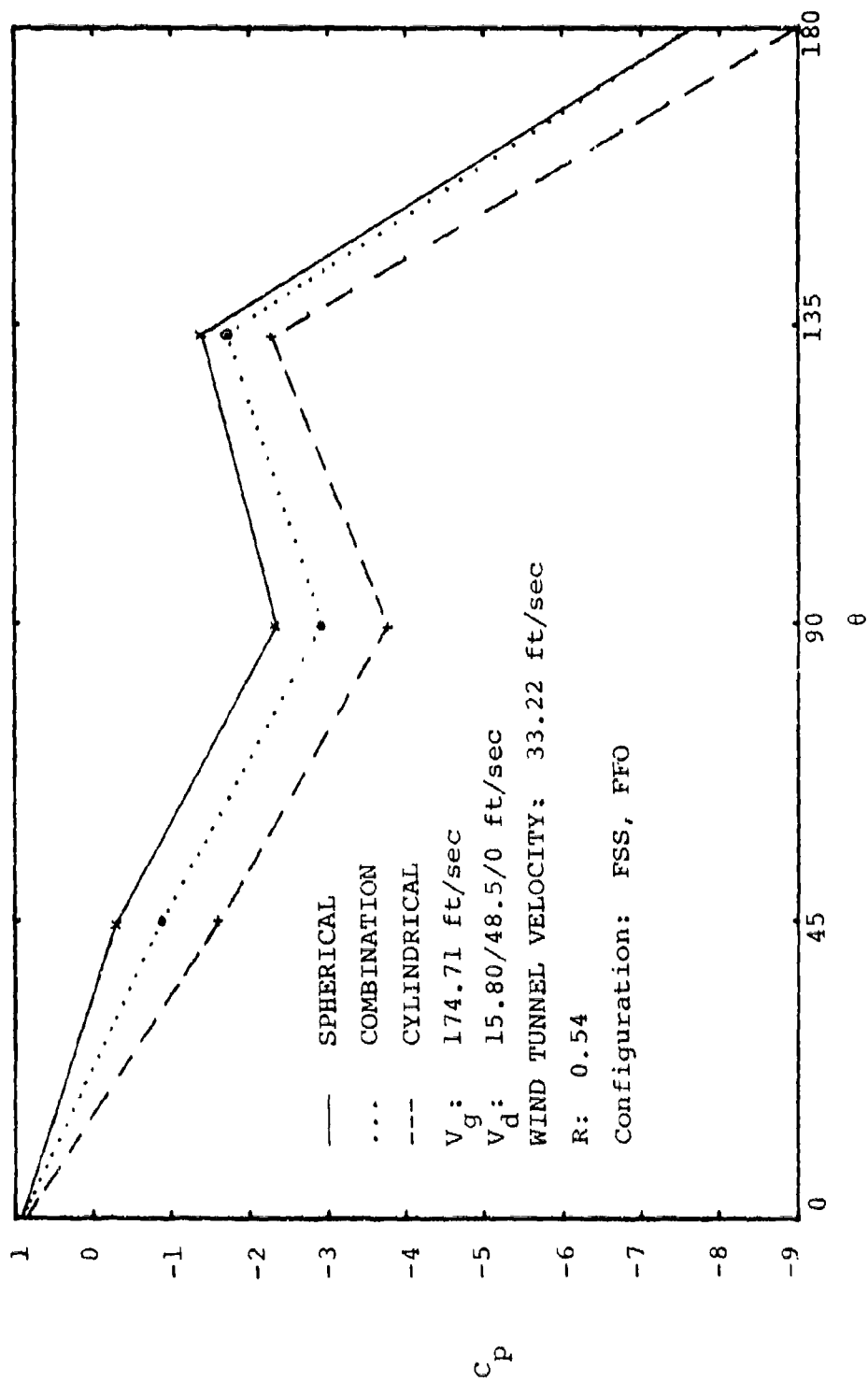


Figure 20. PRESSURE DISTRIBUTION SIDE FUSELAGE
SUCTION; FAIRING FULL OFFSET

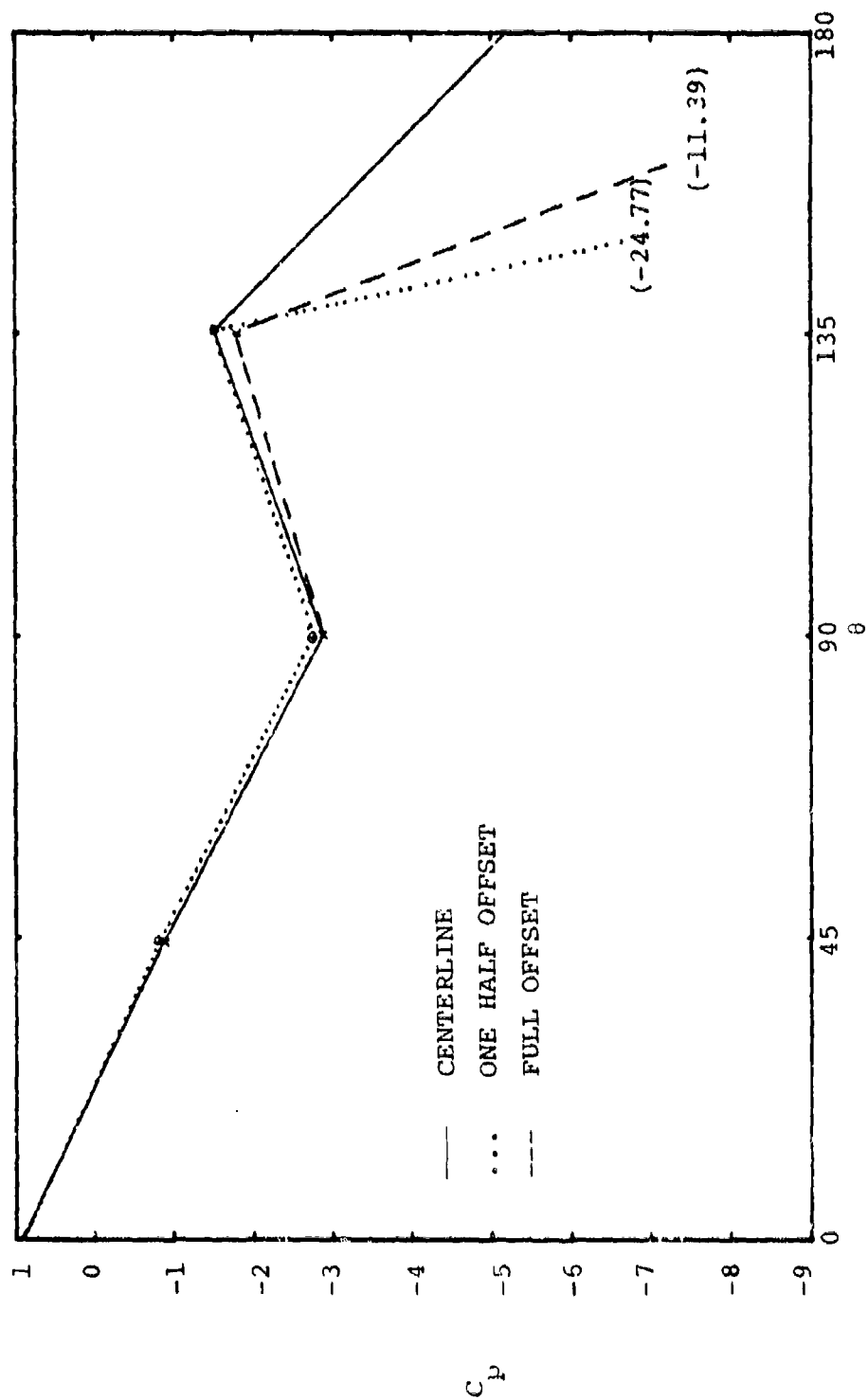


Figure 21. COMBINATION SPHERICAL AND CYLINDRICAL PRESSURE DISTRIBUTION, WITHOUT FUSELAGE SUCTION, ON SIDE IN DIRECTION OF OFFSET

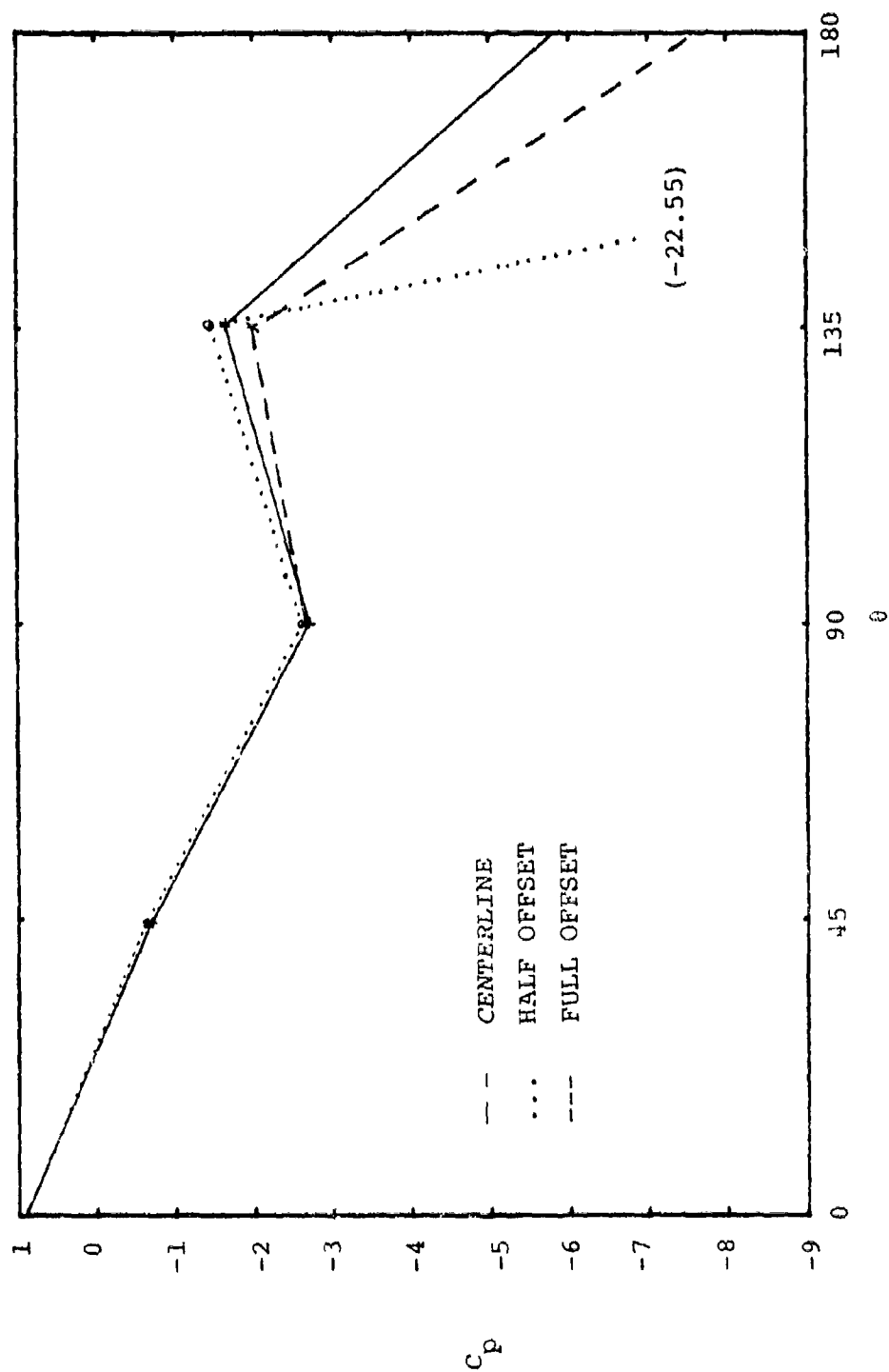


Figure 22. COMBINATION SPHERICAL AND CYLINDRICAL PRESSURE DISTRIBUTION, SIDE FUSELAGE SUCTION, ON SIDE IN DIRECTION OF OFFSET

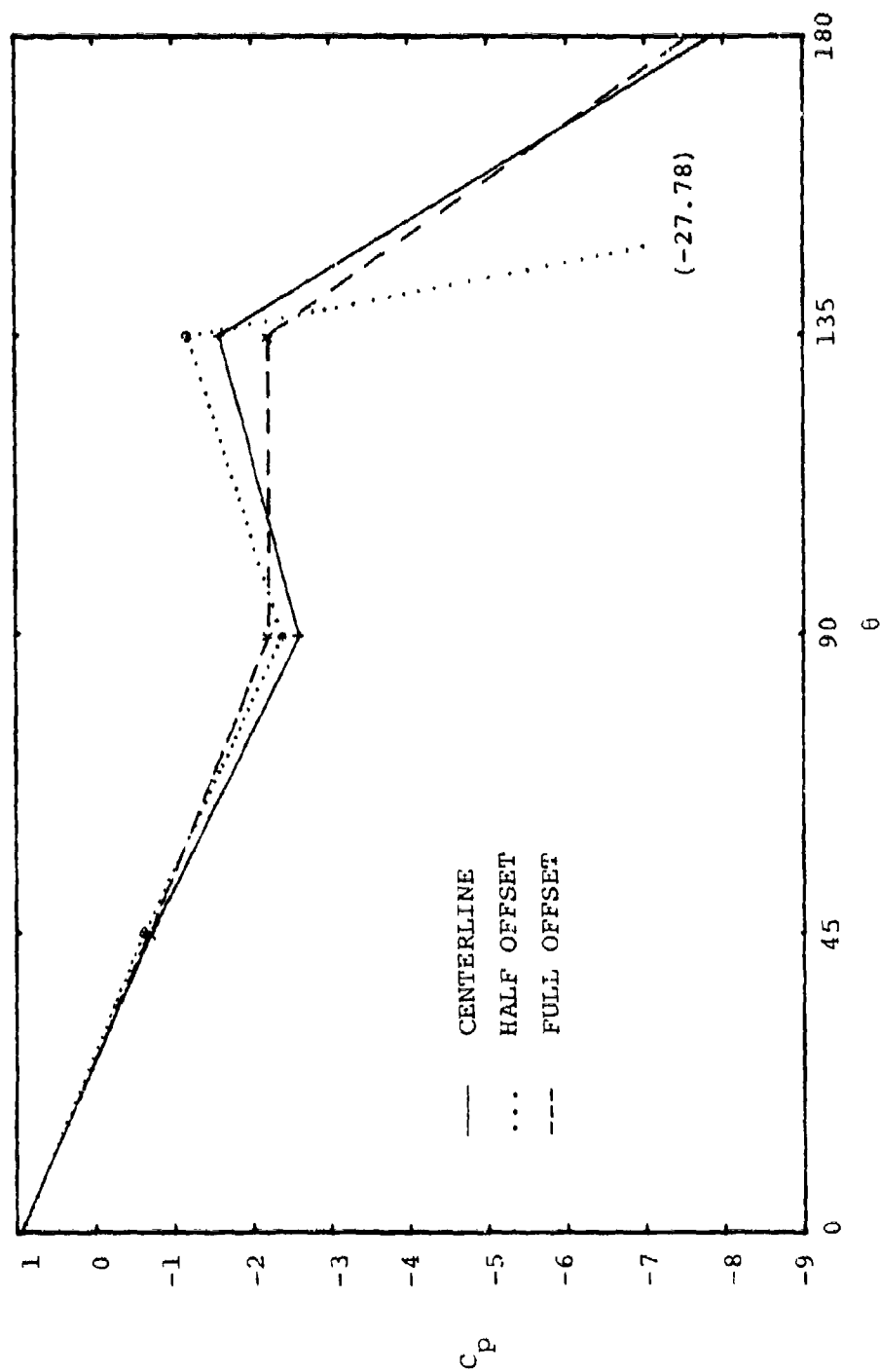


Figure 23. COMBINATION SPHERICAL AND CYLINDRICAL PRESSURE DISTRIBUTION, FUSELAGE SUCTION FORWARD, ON SIDE IN DIRECTION OF OFFSET

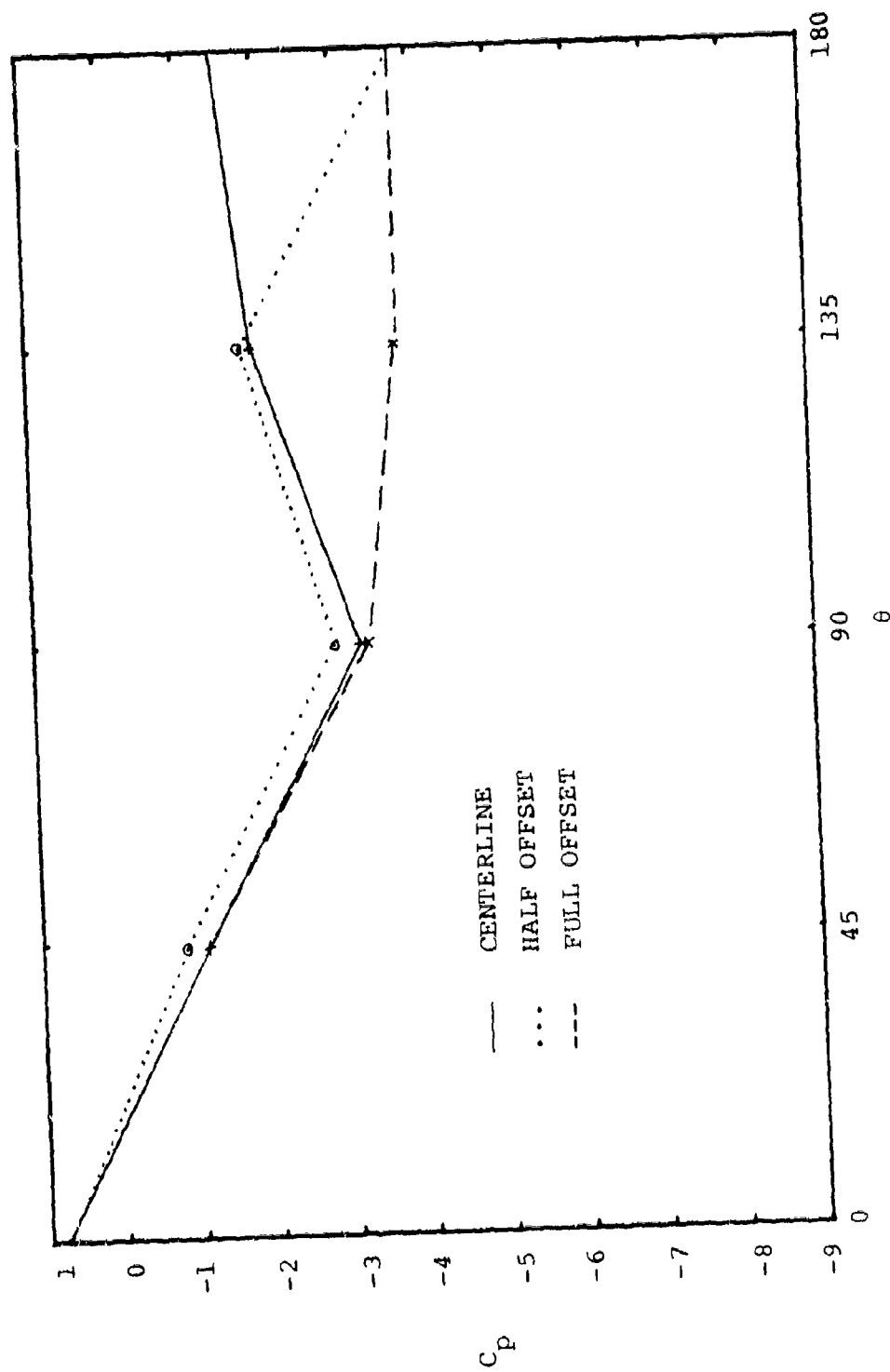


Figure 24. COMBINATION SPHERICAL AND CYLINDRICAL PRESSURE DISTRIBUTION, FUSELAGE SUCTION AFT, ON SIDE IN DIRECTION OF OFFSET

TABLE I
PRESSURE TAP--SCANIVALVE LOCATIONS

<u>PORT #</u>	<u>LOCATION</u>	<u>PORT #</u>	<u>LOCATION</u>
1-11	Ambient Air	29	Turret Hemisphere $\theta = 45^\circ, \phi = 0^\circ$
12	Tunnel Wall-- Dynamic Probe	30	Turret Hemisphere $\theta = 90^\circ, \phi = 0^\circ$
13	Tunnel Wall-- Static (Fore)	31	Turret Hemisphere $\theta = 135^\circ, \phi = 0^\circ$
14	Tunnel Wall--Static	32	Turret Hemisphere $\theta = 180^\circ, \phi = 0^\circ$
15	Tunnel Wall--Static	33	Turret Hemisphere $\theta = 225^\circ, \phi = 0^\circ$
16	Tunnel Wall--Static	34	Turret Hemisphere $\theta = 270^\circ, \phi = 0^\circ$
17	Tunnel Wall--Static	35	Turret Hemisphere $\theta = 315^\circ, \phi = 0^\circ$
18	Tunnel Wall-- Static (Aft)	36	Turret Cylinder $\theta = 0^\circ$
19	Turret Top	37	Turret Cylinder $\theta = 45^\circ$
20	Turret Hemisphere $\theta = 0^\circ, \phi = 45^\circ$	38	Turret Cylinder $\theta = 90^\circ$
21	Turret Hemisphere $\theta = 45^\circ, \phi = 45^\circ$	39	Turret Cylinder $\theta = 135^\circ$
22	Turret Hemisphere $\theta = 90^\circ, \phi = 45^\circ$	40	Turret Cylinder $\theta = 180^\circ$
23	Turret Hemisphere $\theta = 135^\circ, \phi = 45^\circ$	41	Turret Cylinder $\theta = 225^\circ$
24	Turret Hemisphere $\theta = 180^\circ, \phi = 45^\circ$	42	Turret Cylinder $\theta = 270^\circ$
25	Turret Hemisphere $\theta = 225^\circ, \phi = 45^\circ$	43	Turret Cylinder $\theta = 315^\circ$
26	Turret Hemisphere $\theta = 270^\circ, \phi = 45^\circ$	44	Ambient Air
27	Turret Hemisphere $\theta = 315^\circ, \phi = 45^\circ$	45	Scanivalve Calibration
28	Turret Hemisphere $\theta = 0^\circ, \phi = 0^\circ$	46-48	Ambient Air

TABLE II
SUMMARY OF RESULTS

<u>Case</u>	<u>Configuration</u>	<u>V_d (ft/sec)</u>	<u>R</u>	<u>V_g (ft/sec)</u>
1	FSO, FCL	0/43.52/0	0.4287	141.44
1	FSO, FHO	0/36.74/0	0.361	136.89
1	FSO, FFO	0/44.34/0	0.4400	141.29
2	FSF, FCL	18.11/32.94/27.48	0.4717	155.64
2	FSF, FHO	19.5/19.75/35.09	0.3683	139.28
2	FSF, FFO	21.15/27.5/28.9	0.4329	145.93
3	FSA, FCL	-----	-----	-----
3	FSA, FHO	-----	-----	-----
3	FSA, FFO	-----	-----	-----
4	FSS, FCL	15.1/47.93/0	0.5279	175.43
4	FSS, FHO	14.3/36.12/0	0.4152	155.90
4	FSS, FFO	15.80/48.5/0	0.5401	174.71

The definition of abbreviations is as follows:

FSO - Fuselage suction off
 FSF - Fuselage suction forward
 FSS - Fuselage suction side
 FSA - Fuselage suction aft
 FCL - Fairing centerline
 FHO - Fairing one-half offset
 FFO - Fairing full offset

APPENDIX A

PRESSURE COEFFICIENT CALCULATION

The pressure coefficient is given by the equation

$$C_p = \frac{\Delta P}{q} = \frac{P_s - P_\infty}{q},$$

where P_s is static pressure at the turret port designated, P is the static pressure in the wind tunnel (Port 14), q is free-stream dynamic pressure (Port 12-Port 14). Writing in terms of scanivalve port locations,

$$C_p = \frac{P_s - P_{14}}{P_{12} - P_{14}}.$$

As a result of the linearity of the calibration equation used in converting the scanivalve output, the calibration factor is cancelled and the pressure coefficient can be obtained using only scanivalve output voltages.

APPENDIX B

SUCTION DUCT VOLTAGE-TO-VELOCITY CONVERSION EQUATIONS

The following second degree curve-fit equations were used to convert voltage received from the propeller anemometers into velocity [Ref. 5]. Figure 3 shows the locations of these suction ducts. Equation 2a was used for the anemometer for the six runs with no fuselage bleed slot and with it forward. 2b was the replacement anemometer after 2a failed during testing. Y is the duct velocity in feet per second and X is voltage in volts of millivots.

$$\text{Duct \#1: } Y = -7.6316E-0.4 \cdot X + 0.3341 \cdot X + 7.9236 \quad (X \text{ in mv})$$

$$\text{Duct \#2a: } Y = -0.1146 \cdot X^2 + 7.0215 \cdot X + 2.1691 \quad (X \text{ in Volts})$$

$$\text{Duct \#2b: } Y = -0.806 \cdot X^2 + 6.9037 \cdot X + 2.4016 \quad (X \text{ in Volts})$$

$$\text{Duct \#3: } Y = -0.1476 \cdot X^2 + 5.5755 \cdot X + 3.2969 \quad (X \text{ in Volts})$$

LIST OF REFERENCES

1. Craig, James R., Ph.D., A Study in Flow Control and Screening Methods for Aircraft Laser Turrets, Final Report, AFWL-TR-80-119, April 1980.
2. deJonckheere, R. and Russel, J.J., USAF/Air Force Weapons Laboratory, Kirtland Air Force Base, New Mexico; and Chou, D.C., The University of New Mexico, Albuquerque, New Mexico, High Subsonic Flowfield Measurements and Turbulent Flow Analysis Around a Turret Protruberence, AIAA 20th Aerospace Sciences Meeting, 11-14 January 1982, Orlando, Florida.
3. Schorberger, Lieutenant James, Flow Control About an Airborne Laser Turret, M.S. Thesis, Naval Postgraduate School, Monterey, California, 1980.
4. Mandigo, Lieutenant Alan, Control of Airflow About a High Energy Laser Turret, M. S. Thesis, Naval Postgraduate School, Monterey, California, 1980.
5. Rippel, Lieutenant Commander David A., Airborne Laser Turret Flow Control: A Parametric Study of Wind Tunnel Model Conditions, M.S. Thesis, Naval Postgraduate School, Monterey, California, December 1981.
6. Burd, Lieutenant James, Flow Control for a High Energy Laser Turret Using Trapped Vortices Stabilized by Suction, M.S. Thesis, Naval Postgraduate School, Monterey, California, December 1981.
7. Fuhs, Allen E. and Fuhs, Susan E., Optical Phase Distortion Due to Compressible Flow Over Laser Turrets, Proceedings of the Aero-Optics Symposium on electro magnetic wave propagation from aircraft, NASA Conference Publication 2121, April 1980.
8. Aero-Optical Phenomena, Edited by Keith G. Gilbert and Leonard J. Otten, Volume 80, pp. 40-77. Progress in Astronautics and Aeronautics, Martin Summerfield, Series Editor-in-Chief, Princeton, Combustion Research Laboratories, Inc., Princeton, New Jersey.
9. deJonckheere, Richard, Control of Turbulent, Separated Airflow About Aircraft Turrets, Workshop conducted at Air Force Weapons Laboratory, Albuquerque, New Mexico, 10 and 11 March 1980.

10. Schlichting, Dr. Herman, Boundary-Layer Theory, pp. 5-24.
McGraw-Hill Book Co., 1968.
11. Fluid Motion Panel of the Aeronautical Research
Committee, Modern Developments in Fluid Dynamics,
Edited by S. Goldstein, New York, Dover Publications,
Inc., 1965.

INITIAL DISTRIBUTION LIST

	No. Copies
1. Defense Technical Information Center Cameron Station Alexandria, Virginia 22314	2
2. Library, Code 0142 Naval Postgraduate School Monterey, California 93940	2
3. Department Chairman, Code 67 Department of Aeronautics Naval Postgraduate School Monterey, California 93940	1
4. Distinguished Professor Allen E. Fuhs Code 67Fu Department of Aeronautics Naval Postgraduate School Monterey, California 93940	2
5. Captain Richard deJonckheere, USAF AFWL/APLB Kirtland Air Force Base New Mexico 87177	7
6. Captain A. Skolnick PMS 405 Naval Sea Systems Command Washington, D.C. 20360	1
7. LCDR Larry E. Penix 4670 Huggins Street San Diego, California 92122	3
8. Peter Bellamy-Knights Department of Mechanics of Fluids Simon Engineering University of Manchester Manchester M139PL United Kingdom	1
9. Ralph Haslund M/S 8H-29 Boeing Aerospace Company Post Office Box 3999 Seattle, Washington 98124	1

10. Dr. R. Kenneth Lobb
2000 N. Beauregard St.
Center for Naval Analyses
Alexandria, VA 22311

1